

## **Response to Reviewer #1**

We thank Reviewer #1 for their valuable and helpful comments. Our responses to the comments are provided below in bold font with the reviewer's comments in italicized font.

*The paper reports a comprehensive study of the climate and air quality impacts of residential solid fuel combustion. The paper reports the first assessment of the impacts of carbonaceous aerosol from residential solid fuel combustion through changes in ice nuclei as well as a comprehensive assessment of aerosol indirect effects through changes in liquid clouds.*

*The paper makes an important contribution to our understanding of residential solid fuel combustion on climate and is suitable for publication in ACP. Importantly the manuscript highlights that the overall climate impact of carbonaceous aerosol from residential solid fuel combustion is uncertain and that even the sign of the impact is still ambiguous. The paper certainly motivates further study of this important issue and highlights where some of the major uncertainties lie.*

*The manuscript is very well written and clear. I only have a few minor comments. I suggest publication in ACP after the following minor comments have been addressed.*

*Minor Comments:*

*Page 5. Have you stated the size of the emitted carbonaceous aerosol? This is important for the impacts of carbonaceous aerosol on cloud condensation nuclei and aerosol indirect effects.*

**Response: We have added the size range of the emitted carbonaceous aerosols in the text (Page 5, Lines 155-156): “Specifically, BC and POM from solid fuel cookstove emissions are treated in the accumulation mode, with size range of 0.058-0.27  $\mu\text{m}$  (Liu et al., 2012).”**

*Page 12. Most models do not simulate the impacts of BC on ice nuclei. I think it would be useful to provide a brief summary of how this was treated in the Methods section of the paper.*

**Response:** We agree with the reviewer. We have moved part of the contents from Section 3.4.4 to a new section in Methods as Section 2.5 and added the description of BC as IN following Barahona and Nenes (2008, 2009) in the text (Page 7, Lines 197-212):

## **2.5 Simulations: BC active as IN**

**“In default CAM5-Chem, BC is not treated as IN (Liu et al., 2012; Tilmes et al., 2015). IN concentrations from homogeneous nucleation are calculated as a function of vertical velocity (Liu et al., 2007). Several lab and field studies indicate that BC particles can act as IN (Cozic et al., 2008; DeMott et al., 1999; Koehler et al., 2009; Kulkarni et al., 2016). Therefore, we conduct additional simulations that treat BC as an effective IN applying the ice nucleation scheme of Barahona and Nenes (2008, 2009). The scheme estimates maximum supersaturation and ice crystal concentrations and considers competition between homogeneous and heterogeneous freezing. Homogeneous nucleation occurs in solution droplets formed on soluble aerosols (mainly sulfate), while heterogeneous nucleation occurs on IN, which here are a small subset of mineral dust and black carbon particles. The heterogeneous freezing of BC and dust is described as a generalized ice nucleation spectrum.**

**We perform three additional model simulations, with model configurations identical to those in Table 2, except for the treatment of BC particles as effective IN. In addition, for each model simulation, we alter the plausible maximum freezing efficiency (MFE) of BC as 0.01, 0.05 and 0.1 that provides an uncertainty range in the global climatic impact assessment.”**

*Page 15. As stated by the authors the aerosol indirect effect is considerably larger than other studies. Ward et al. (2012) also found a large aerosol indirect effect using the CAM model (although a different version) to study carbonaceous aerosol from fires. It might be useful to point this out in the text.*

**Response:** We have added (Page 16, Lines 489-490): “Consistent with our study, Ward et al. (2012) also found a large AIE (-1.74 to 1.00 W m<sup>-2</sup>) for carbonaceous aerosols from fires using CESM CAM4-Chem.”

*Fig. 4 and 5. Please clarify whether these are reported at ambient conditions or at standard temperature and pressure.*

**Response:** We have clarified the reporting units for BC and POM under standard temperature and pressure, which have been added in the caption of Fig. 4 as (Page 36, Lines 916-917) “Figure 4. Annual zonal mean BC concentrations from (a) the BASE simulation, (b) the global and (c) India solid fuel cookstove emissions. BC concentrations are calculated under standard temperature and pressure conditions (273 K, 1 atm).”

## **Response to Reviewer #2**

We thank Reviewer #2 for their valuable and helpful comments. Our responses to the comments are provided below in bold font with the reviewer's comments in italicized font.

*The manuscript by Huang et al. presents a modeling study of the radiative effects of solid fuel cookstoves, both globally and specifically in India. There is a lot of scientific and policy interest in this topic, given the potential climate co-benefits of cookstove intervention programs and the uncertainty associated with quantifying this, with several recent papers making a range of estimates that differ in sign. The contribution of this article is a welcome addition to the field, focusing particularly on details of aerosol cloud interactions, and considering the effect of BC ice nucleation, which has not been considered in such studies previously. Overall the manuscript is thus appropriate in scope for ACP. It is also generally clear, well organized, and easy to read. I only have a few comments that are detailed below; there is some ambiguity regarding how the authors are arriving at their uncertainty estimates, and some of the motivation for the scope of their analysis (e.g., considering just India, or not considering the impact of co-emitted GHGs) could be strengthened. Addressing these would constitute minor revision.*

### *Major Comments:*

*37: An important conclusion, which I mainly agree with in spirit. However, it might be stated a little bit softer for a few reasons. First, the uncertainty of up to a factor of two in estimating concentrations would seem to contribute to the overall uncertainty in the net radiate effects. Second, this study is of radiative effects, not the climate response, and the wording should reflect that. Third, it's the result of only a single model, which may not be as definitive as presented.*

**Response:** We prefer to keep the original statement as is. First, the manuscript includes a comparative description of all previous results with several different global aerosol-climate model frameworks that supports the uncertain sign conclusion for net global radiative effect of cookstove aerosol emissions. Second, the statement clearly refers to carbonaceous aerosols only and highlights the need for improved constraints on aerosol-cloud interactions. Finally, our study quantifies the impacts of cookstove carbonaceous aerosol emissions on global average annual mean radiative effect because it is a linear predictor of

global average surface air temperature response at equilibrium. Our community is still several years away from any quantitative robust mechanistic understanding of regional climate response to regional radiative effect of aerosols (e.g. Kasoar et al., ACP, 2016). It would be fairly pedagogical to convert the global radiative effect results to global average surface air temperature response e.g. Berntsen and Fuglestad, PNAS, 2008.

*The measurements used for comparison come from very different time periods (2010 for IMPROVE, 2009-2013 for Europe, 2000-2008 for AMS data, and 1993-2016 for AERONET). How does this impact the evaluation of modeled concentrations and AOD, given that the model uses emissions from 2010 and that there have been large changes in emissions over this time period?*

**Response:** The measurement data availability and model configuration has necessitated using climatological observations for BC, OA and AOD with some apparent mismatches between observational years and simulations years for OA and AOD. Model simulated BC concentrations were sampled in exact correspondence to the observed temporal period. The global aerosol-climate model framework is a chemistry-climate model with specified dynamics (CCM-SD), not a chemistry transport model (CTM). CTMs exist to compare with exact measurement periods. In our case, the model output reflects a present-day climatology rather than a specific CTM run year as such. Therefore, the comparison with available climatological measurements does allow us to validate and have insights into the large-scale aerosol system dynamics and behavior. We clarify in the text (Pages 14-15, Lines 429-436): “The simulations reflect a present-day climatology forced with recycled year 2010 anthropogenic emissions. Model simulated BC concentrations were sampled in exact correspondence to the observed temporal period. In some limited cases, OA and AOD are not exactly temporally consistent with the available aerosol measurement network climatologies applied in the evaluation. For regions where carbonaceous aerosol emissions have undergone substantial changes over short periods, the model-measurement comparison may therefore introduce additional uncertainty. However, we focus the evaluation on the large-scale regional aerosol system dynamics.”

215 - 220: *Some previous studies have suggested that the resolution of global scale models leads to a bias that makes it difficult to match AOD from AERONET in these regions. Could this partially explain the low bias?*

**Response:** We agree and have added (Page 9, Lines 257-259): “The model underestimate of AOD from AERONET in India may also be related to the fairly coarse global model resolution, as previously reported by Pan et al. (2015) and Zhang et al. (2015).”

*Fig 6 and Section 3.4.1 (and everywhere these numbers are quoted in the text): Suddenly the results have errors associated with them (concentrations and AOD did not: : :). What is the meaning of the error estimates? Are these the standard deviations over the timeframe modeled? If so, that needs to be more clearly stated when presenting these numbers in the abstract and conclusion (that +/- is modeled temporal standard deviation). And then I wonder why similar deviations were not considered for discussion of concentrations or AOD. Further, temporal variability is very different than e.g. an estimate of uncertainty owing to sources of model error or approximations, such as the ranges provided for the RF of the simulations including BC IN that stem from uncertainty in the MFE. These ranges can't be directly compared, and yet they're presented in e.g. the abstract without distinguishing their different meanings. At present the non BC-IN ranges come across as uncertainty estimates that seem much too small (I doubt the authors believe that the aerosol RF in any single model could be that accurate).*

**Response:** We include uncertainty estimates that are based on interannual internal climate variability (n=5 years). For consistency, we have added the uncertainty ranges based on interannual internal climate model variability to concentrations and burdens of BC and POM, and AOD where multiple years have been sampled for the comparison. For example, model BC concentrations were sampled in correspondence to the exact temporal measurement period, thus no range included for that case. This revision is reflected throughout the updated manuscript, in the abstract, Section 3.1, Section 3.2, Section 3.3 and Section 4 e.g. (Page 1, Lines 24-26): “However, the model tends to underestimate AOD over India and China by  $\sim 19 \pm 4\%$  but overestimate it over Africa by  $\sim 25 \pm 11\%$

(uncertainty range due to interannual internal climate model variability for n=5 run years).”

(Pages 8-9, Lines 239-244): “Figure 2 shows the evaluation of simulated surface OA against observations. Over East Asia, the model slightly underestimates observed OA, with a NMB of  $-8.5 \pm 5\%$  (Fig. 2a). In contrast, the simulated OA concentrations overestimate the measurements by over a factor of 2 in North America, with a NMB value of  $124 \pm 24\%$  (Fig. 2b). For the European sites, we find a simulated OA overestimation of measured concentrations by up to  $0.9 \pm 0.7 \mu\text{g m}^{-3}$ , corresponding to a NMB of  $+32 \pm 26\%$  (Fig. 2c).”

(Page 9, Lines 248-250): “Over India, the simulated annual mean AOD is lower than observations by about  $16 \pm 3\%$  (Fig. 3a), with large bias sources mainly from the northern India regions (e.g., New Delhi and Kanpur).”

(Page 9, Lines 259-261): “A similar pattern is found over China (Fig. 3b) and the rest of Asia (Fig. 3c), with NMB values of  $-21 \pm 4\%$  and  $-15 \pm 6\%$  respectively.”

(Page 9, Lines 263-265): “This directly leads to annual mean model simulated AOD values over Africa  $25 \pm 11\%$  higher than observations because Saharan dust emissions dominate the AOD over North Africa (Fig. 3d).”

(Pages 9-10, Lines 270-274): “In these two regions, modeled AOD agrees with observations within a factor of 2, with NMB values  $-20 \pm 4\%$  and  $-18 \pm 9\%$  respectively. CAM5-Chem overestimates AOD over Australia (Fig. 3h) and remote sites (Fig. 3i), with NMB values of  $+69 \pm 17\%$  and  $+47 \pm 12\%$ , respectively. Globally, model simulated AOD agrees quite well with observations, with NMB values close to zero.”

(Page 10, Lines 279-282): “For the control simulation, global annual mean BC burden and lifetime are  $0.12 \pm 0.001 \text{ Tg}$  and  $4.5 \pm 0.04 \text{ days}$ , respectively (Table 3), at the low end of the range estimated by AeroCom (Schulz et al., 2006; Textor et al., 2006).”

(Page 10, Lines 290-292): “Annual mean BC burdens from global and Indian solid fuel cookstove emissions account for about  $24.2 \pm 0.7\%$  and  $5.0 \pm 0.0\%$  of that in the control simulation ( $0.12 \pm 0.001 \text{ Tg}$ ).”

(Page 10, Lines 296-298): “In our control simulation, the annual mean POM burden is  $0.66 \pm 0.006 \text{ Tg}$ , and the global annual mean POM lifetime is  $4.8 \pm 0.04 \text{ days}$  (Table 3).”

**(Page 11, Lines 307-308): “The annual mean POM burdens from global and Indian solid fuel cookstove emissions are  $0.13 \pm 0.004$  Tg and  $0.027 \pm 0.002$  Tg respectively.”**

**(Page 15, Lines 436-442): “In the control simulation, the global annual mean BC burden and lifetime are  $0.12 \pm 0.001$  Tg and  $4.5 \pm 0.04$  days. For POM, the burden and lifetime are  $0.66 \pm 0.006$  Tg and  $4.8 \pm 0.04$  days. Annual mean surface BC (POM) concentrations over Northern India, East China and sub-Saharan Africa are  $1.55 \pm 0.076$ ,  $0.76 \pm 0.028$  and  $0.11 \pm 0.004 \mu\text{g m}^{-3}$  ( $7.11 \pm 0.32$ ,  $3.95 \pm 0.12$  and  $0.48 \pm 0.02 \mu\text{g m}^{-3}$ ), respectively. BC and POM burdens from global solid fuel cookstove emissions are  $0.029 \pm 0.001$  and  $0.13 \pm 0.004$  Tg, while contributions from the Indian sector are  $0.006 \pm 0.000$  and  $0.027 \pm 0.004$  Tg, respectively.”**

**We have clarified in the abstract and text to distinguish the 2 uncertainty range calculations used in the study (1) based on interannual internal climate model variability (2) based on BC maximum freezing efficiency range (Page 2, Lines 38-39):**

**“Here, the uncertainty range is based on sensitivity simulations that alter the maximum freezing efficiency of BC across a plausible range: 0.01, 0.05 and 0.1.”**

**(Page 7, Lines 209-212): “We perform three additional model simulations, with model configurations identical to those in Table 2, except for the treatment of BC particles as effective IN. In addition, for each model simulation, we alter the plausible maximum freezing efficiency (MFE) of BC as 0.01, 0.05 and 0.1 that provides an uncertainty range in the global climatic impact assessment.”**

*Introduction: I didn't get a good sense from the introduction why there is a particular interest in India as separate from the globe in this study (as opposed to China, or any other country with significant cookstove use). I'm not suggesting that the authors do more simulations for other regions, but if they wish to include the India-specific results it would make more sense to include a bit more rational for this emphasis.*

**Response: We have expanded the India regional focus motivation statement (Page 2, Lines 53-61):**



**“India contains a large concentration of solid fuel-dependent households: approximately 160 million households use solid fuels for cooking (Venkataraman et al., 2010). In India, residential biofuel combustion represents the dominant energy sector and accounts for over 50% of the total source of BC and OC emissions (Klimont et al., 2009). India has a long history of unsuccessful stove intervention programs that have sometimes focused on health benefits (Hanbar and Karve, 2002; Kanagawa and Nakata, 2007; Kishore and Ramana, 2002). Despite years of interventions, the vast majority of Indian households still rely on traditional stoves (Legros et al., 2009). The possible scope for global climate co-benefits in future Indian cookstove intervention programs warrants further examination and analysis of this region.”**

*439 - 447: I think it's worth recognizing that there are climate impacts from GHG emissions as well. So, considering not just the aerosol emissions, these may be large enough to make the net climate images of cookstove emissions positive (Lacey 2017). It is somewhat artificial to envision a scenario wherein only the carbonaceous aerosol cookstove emissions are effected by stove replacements.*

**Response: We have added (Page 17, Lines 508-510) “This study does not include the greenhouse gas emission effects from the solid fuel cookstove sector, which may indeed be large enough to imply a net warming global climate impact depending on time scale (Lacey et al., 2017).”**

*Minor Comments:*

*12: Not clear – “updated” related to what? A particular previous study? Later it becomes evident what is meant (first to include BC as IN), but perhaps it could be worded differently here.*

**Response: We have deleted “updated”.**

*74: Clarify whether the Butt 2016 study included just aerosols or also GHGs in the DRE.*

**Response: We have clarified (Page 3, Lines 86-88): “Butt et al. (2016) reported that the net DRE and AIE of aerosols from the residential emission sector (including coal) ranged from -66 to +21 mW m<sup>-2</sup>, and from -52 to -16 mW m<sup>-2</sup>, respectively. Their study did not include greenhouse gases.”**

80: *Similarly, Ethiopia is the 3rd largest in Lacey 2017, but that's including GHGs in 2050, which is a slightly more specific statement than as presented here.*

**Response:** We have revised to (Pages 3-4 Lines 89-95) “From the perspective of policy-relevant country-level assessment of cookstove burning on global climate, Lacey and Henze (2015) revealed that solid fuel cookstove aerosol emissions resulted in global air surface temperature changes ranging from 0.28 K cooling to 0.16 K warming; Lacey et al. (2017) further concluded that emissions reductions, including both aerosols and greenhouse gases, from China, India and Ethiopia contributed the most to the global surface temperature changes by 2050.”

128: *CAM5-Chem not CAM5-chem*

**Response:** Corrected.

*Fig 1: Sorry if I just missed it, but did the authors state how they are defining urban vs rural in their classification of measurement sites?*

**Response:** We have added the definition of the classification of urban and rural sites in the text as (Page 5 Lines 128-129) “Here we define urban (including semi-urban) sites as the geographic locations of the measured sites locating in a city, others as rural sites.”

276-279: *What is the BC mass absorption coefficient (MABS) at 550 nm in this model? See e.g. Koch ACP 2009*

**Response:** BC mass absorption cross section coefficient at 550 nm in CAM5-Chem is  $14.6 \text{ m}^2 \text{ g}^{-1}$ . We have updated this in the revised text as (Page 11 Lines 319-323) “CAM5-Chem assumes that BC is internally mixed with other components in the accumulation mode and simulates enhanced absorption (BC mass absorption cross section =  $14.6 \text{ m}^2 \text{ g}^{-1}$ ) when BC is coated by soluble aerosol components and water vapor (Ghan et al., 2012), which results in larger estimates of the DRE than for BC alone (Bond et al., 2013; Jacobson, 2001b).”

# Global radiative effects of solid fuel cookstove aerosol emissions

Yaoxian Huang<sup>1,a</sup>, Nadine Unger<sup>2</sup>, Trude Storelvmo<sup>3</sup>, Kandice Harper<sup>1</sup>, Yiqi Zheng<sup>3</sup>, and Chris Heyes<sup>4</sup>

<sup>1</sup>School of Forestry and Environmental Studies, Yale University, New Haven, CT 06511, USA

<sup>2</sup>College of Engineering, Mathematics and Physical Sciences, University of Exeter, Exeter, EX4 4QE, UK

<sup>3</sup>Department of Geology and Geophysics, Yale University, New Haven, CT 06511, USA

<sup>4</sup>International Institute for Applied Systems Analysis, Laxenburg, Austria

<sup>a</sup>now at: [Department of Climate and Space Sciences and Engineering, University of Michigan, Ann Arbor, MI 48109, USA](#)

Correspondence to: Yaoxian Huang ([yaoxian.huang1@gmail.com](mailto:yaoxian.huang1@gmail.com))

**Abstract.** We apply the NCAR CAM5-Chem global aerosol-climate model to quantify the net global radiative effects of black and organic carbon aerosols from global and Indian solid fuel cookstove emissions for the year 2010. Our assessment accounts for the direct radiative effects, changes to cloud albedo and lifetime (aerosol indirect effect, AIE), impacts on clouds via the vertical temperature profile (semi-direct effect, SDE), and changes in the surface albedo of snow and ice (surface albedo effect). In addition, we provide the first estimate of household solid fuel black carbon emission effects on ice clouds. Anthropogenic emissions are from the IIASA GAINS ECLIPSE V5a inventory. A global dataset of black carbon (BC) and organic aerosol (OA) measurements from surface sites and aerosol optical depth (AOD) from AERONET is used to evaluate the model skill. Compared with observations, the model successfully reproduces the spatial patterns of atmospheric BC and OA concentrations, and agrees with measurements to within a factor of 2. Globally, the simulated AOD agrees well with observations, with normalized mean bias close to zero. However, the model tends to underestimate AOD over India and China by  $\sim 19 \pm 4\%$  but overestimate it over Africa by  $\sim 25 \pm 11\%$  (uncertainty range due to interannual internal climate model variability for  $n=5$  run years). Without BC serving as ice nuclei (IN), global and Indian solid fuel cookstove aerosol emissions have a net cooling impact on global climate of  $-141 \pm 4 \text{ mW m}^{-2}$  and  $-12 \pm 4 \text{ mW m}^{-2}$ , respectively. The net radiative impacts are dominated by the AIE and SDE mechanisms, which originate from enhanced cloud condensation nuclei

Deleted: .

Deleted: yale.edu

Deleted: updated

concentrations for the formation of liquid and mixed-phase clouds, and a suppression of convective transport of water vapor from the lower troposphere to the upper troposphere/lower stratosphere that in turn leads to reduced ice cloud formation. When BC is allowed to behave as a source of IN, the net global climate impacts of the global and Indian solid fuel cookstove emissions range from -275 to +154 mW m<sup>-2</sup> and -33 to +24 mW m<sup>-2</sup>, with globally averaged values -59 ± 215 and 0.3 ± 29 mW m<sup>-2</sup> respectively. Here, the uncertainty range is based on sensitivity simulations that alter the maximum freezing efficiency of BC across a plausible range: 0.01, 0.05 and 0.1. BC-ice cloud interactions lead to substantial increases in high cloud (< 500 hPa) fractions. Thus, the net sign of the impacts of carbonaceous aerosols from solid fuel cookstoves on global climate (warming or cooling) remains ambiguous until improved constraints on BC interactions with mixed-phase and ice clouds are available.

## 1. Introduction

Worldwide 2-3 billion people rely on solid fuels for the majority of their energy needs (Legros et al., 2009). This household biomass combustion includes burning wood fuel, agricultural residues and dung for cooking, heating and lighting. Emissions from household solid fuel combustion include greenhouse gases (carbon dioxide and methane), black carbon (BC), organic carbon (OC), and other trace gases (e.g., nitrogen oxides). Globally, BC from household solid fuel emissions accounts for approximately 25% of the total anthropogenic BC emissions (Bond et al., 2013). Among different types of cookstoves, advanced charcoal stoves show lowest BC emission factors, followed by simple charcoal, advanced biomass, rocket and simple wood stoves, respectively (Garland et al., 2017). India contains a large concentration of solid fuel-dependent households: approximately 160 million households use solid fuels for cooking (Venkataraman et al., 2010). In India, residential biofuel combustion represents the dominant energy sector and accounts for over 50% of the total source of BC and OC emissions (Klimont et al., 2009). India has a long history of unsuccessful stove intervention programs that have sometimes focused on health benefits (Hanbar and Karve, 2002; Kanagawa and Nakata, 2007; Kishore and Ramana, 2002). Despite years of interventions, the vast majority of Indian households still rely on traditional stoves (Legros et al., 2009). The possible scope for global climate co-benefits in future Indian cookstove intervention programs warrants further examination and analysis of this region. BC-rich household solid fuel emission plays an important role in affecting regional air quality (Archer-Nicholls et al.,

63 2016; Carter et al., 2016; Liu et al., 2016) and influencing global climate change (Bauer et al.,  
64 2010; Butt et al., 2016; Venkataraman et al., 2005). The human health consequences of solid fuel  
65 combustion are substantial (Archer-Nicholls et al., 2016; Ezzati and Kammen, 2002; Lelieveld et  
66 al., 2015). Nearly 9% of the global burden of disease is attributable to exposure to household air  
67 pollution from solid fuels, equivalent to 2.9 million premature deaths and 86 million disability  
68 adjusted life years (DALYs) annually (GBD 2015 Risk Factors Collaborators, 2016). Half of the  
69 world's population is exposed to indoor air pollution, mainly attributable to solid fuel usage for  
70 household cooking and heating (Bonjour et al., 2013; Smith et al., 2014).

71 Carbonaceous aerosols from solid fuel combustion interact with the Earth's radiation budget  
72 directly by absorbing and scattering solar radiation (direct radiative effect, DRE) and indirectly by  
73 changing cloud albedo and lifetime (aerosol indirect effect, AIE), modifying the vertical  
74 temperature profile (semi-direct effect, SDE), and changing the surface albedo over snow and ice  
75 (surface albedo effect, SAE) (Boucher et al., 2013; Chung, 2005; Chylek and Wong, 1995; Ghan,  
76 2013; Ghan et al., 2012; Myhre et al., 2013). Carbonaceous aerosols affect cloud albedo and  
77 lifetimes (the AIE) by acting as cloud condensation nuclei (CCN) or ice nuclei (IN), thus  
78 modifying cloud properties and changing the top-of-atmosphere (TOA) radiative fluxes  
79 (Lohmann, 2002; Lohmann et al., 2000; Penner et al., 1992; Pierce et al., 2007; Spracklen et al.,  
80 2011b). The net climatic effect of carbonaceous aerosols from household solid fuel combustion is  
81 not well constrained and even the sign is uncertain (Bond et al., 2013). Bauer et al. (2010)  
82 estimated that the aerosol net global climate impact of residential biofuel carbonaceous aerosol  
83 emissions is  $-130 \text{ mW m}^{-2}$ . Kodros et al. (2015) have estimated that net DRE of solid fuel aerosol  
84 emissions ranges from  $-20$  to  $+60 \text{ mW m}^{-2}$ , AIE from  $-20$  to  $+10 \text{ mW m}^{-2}$ , with uncertainties due to  
85 assumptions of the aerosol emission masses, size distribution, aerosol optical properties and  
86 mixing states. Butt et al. (2016) reported that the net DRE and AIE of aerosols from the residential  
87 emission sector (including coal) ranged from  $-66$  to  $+21 \text{ mW m}^{-2}$ , and from  $-52$  to  $-16 \text{ mW m}^{-2}$ ,  
88 respectively. Their study did not include greenhouse gases. Moreover, neither of the latter two  
89 studies consider the aerosol cloud-lifetime effect (second indirect effect), SDE and SAE. From the  
90 perspective of policy-relevant country-level assessment of cookstove burning on global climate,  
91 Lacey and Henze (2015) revealed that solid fuel cookstove aerosol emissions resulted in global air  
92 surface temperature changes ranging from  $0.28 \text{ K}$  cooling to  $0.16 \text{ K}$  warming; Lacey et al. (2017)

Deleted: However

94 ~~further concluded~~ that emissions ~~reductions, including both aerosols and greenhouse gases~~, from  
95 China, India and Ethiopia contributed the most to the global surface temperature changes ~~by 2050~~.

Deleted: ,

Deleted: ing

Deleted: (Lacey et al., 2017)

96 None of the previous assessments have included BC-ice cloud interactions that can exert a large  
97 influence on the atmospheric radiation balance. A recent study by Kulkarni et al. (2016) showed  
98 that BC could act as IN, which was also shown by past lab and field findings (Cozic et al., 2008;  
99 DeMott et al., 1999; Koehler et al., 2009). With BC as IN, Penner et al. (2009) estimated that the  
100 total radiative forcing of anthropogenic and biomass BC emissions was -300 to -400 mW m<sup>-2</sup>, with  
101 IN parameterizations following Liu and Penner (2005) and Kärcher et al. (2006). Gettelman et al.  
102 (2012) further concluded that AIE from BC emissions was -60 mW m<sup>-2</sup>, with ~~ice nucleation~~,  
103 parameterization following Barahona and Nenes (2009). Hence, a re-assessment of the global  
104 climate change impacts of carbonaceous aerosol emissions from the solid fuel cookstove sector  
105 that newly incorporates BC as IN is urgently needed.

Deleted: IN

106 Here, we employ a global aerosol-climate model to quantify the impacts of solid fuel cookstove  
107 carbonaceous aerosol emissions globally and from India on global climate change. Sect. 2 presents  
108 the Methods including the evaluation measurement data sets for BC, OA and aerosol optical depth  
109 (AOD), the model description and experimental design. Sect. 3 details the results of the model  
110 evaluation and the impacts of the global and Indian solid fuel cookstove emissions on the  
111 atmospheric radiation budget and global climate. Discussion and summary are provided in Sect.  
112 4.

## 113 2. Methods

### 114 2.1 BC and OC evaluation measurement database

116 Ground-based BC observations are from IMPROVE (the Interagency Monitoring of PROtected  
117 Visual Environment, <http://vista.cira.colostate.edu/Improve/>) for the year 2010 over North  
118 America (Malm et al., 1994), EMEP (the European Monitoring and Evaluation Programme,  
119 <http://ebas.nilu.no>) for 2009-2013 over Europe, and sporadic measurement campaigns for China  
120 and India. Elemental carbon (EC) concentrations are measured using Thermal Optical Reflectance  
121 (TOR) (Chow et al., 1993, 2004; EMEP/MSC-W et al., 2014). Our measurement database  
122 comprises a total of 152 sites from IMPROVE, 28 sites from EMEP, 35 sites for China, and 41  
123 sites for India. The number of urban sites includes 8 from IMPROVE, 5 from EMEP, 17 for China,

and 23 for India. Here we define urban (including semi-urban) sites as the geographic locations of the measured sites locating in a city, others as rural sites.

A global network of aerosol mass spectrometer (AMS) surface measurements for organic aerosol (OA) for 2000-2008 are used to compare with model simulations (Spracklen et al., 2011a; Zhang et al., 2007; Zheng et al., 2015). The AMS technique measures hydrocarbon-like OA (HOA), oxygenated OA (OOA) and total OA (HOA + OOA). HOA is a surrogate for primary OA (POA) emitted directly from fossil fuel and biomass burning, while OOA is a surrogate for secondary OA (SOA). In this study, we compare monthly mean total OA with model simulated total OA (POA + SOA). The majority of the AMS measurements in the surface concentration database were made prior to 2005.

Ground-based AOD observations from AERONET (AErosol RObtic NETwork, <https://aeronet.gsfc.nasa.gov>) during 1993-2016 are applied to examine model skill (Dubovik and King, 2000; Holben et al., 1998, 2001). A climatological AOD value averaged over 1993-2016 for each site is used to compare with the model simulation. The AERONET version 2 level-2 product is used in this study.

## 2.2 NCAR CAM5-Chem global model description

We apply the NCAR Community Atmosphere Model version 5.3 with chemistry (CAM5-Chem) within the Community Earth System Model (CESM) version 1.2.2 (Emmons et al., 2010; Lamarque et al., 2012; Tilmes et al., 2015). The oxidant-aerosol system is fully coupled in CAM5-Chem. The horizontal resolution of CAM5-Chem is 0.9° latitude by 1.25° longitude, with 56 vertical levels from surface up to about 40 km. In the standard CAM5-Chem, aerosol microphysical processes are represented using a 3-mode scheme (MAM3; aiten, accumulation and coarse modes). MAM3 simulates both mass and number concentrations of aerosols. Aerosol size distributions in each mode are assumed to be lognormal (Liu et al., 2012). The model treats the effects of aerosol acting as CCN in liquid-phase clouds (Ghan et al., 2012). The aerosol components in MAM3 include BC, primary organic matter (POM), secondary organic aerosol (SOA), sulfate, sea salt and dust, which are assumed to be internally mixed within each lognormal mode. Specifically, BC and POM from solid fuel cookstove emissions are treated in the accumulation mode, with size range of 0.058-0.27  $\mu\text{m}$  (Liu et al., 2012). Mass yields of semi-

Deleted: c

158 volatile organic gas-phase species (SOAG) from emissions of isoprene, monoterpenes, big alkanes  
159 and alkenes, as well as toluene are prescribed (Emmons et al., 2010; Liu et al., 2012; Tilmes et al.,  
160 2015). The condensable SOAG reversibly and kinetically partitions into the aerosol phase to form  
161 SOA in CAM5-Chem as described in Liu et al. (2012).

## 162 **2.3 Emissions**

163 Global anthropogenic emissions are from the IIASA (International Institute for Applied System  
164 Analysis) Greenhouse Gas-Air Pollution Interactions and Synergies (GAINS) integrated  
165 assessment model ECLIPSE V5a (Evaluating the Climate and Air Quality Impacts of Short-lived  
166 Pollutants version 5a) for the year 2010 (Amann et al., 2011, 2013; Klimont et al., 2017; Stohl et  
167 al., 2015). Species in ECLIPSE V5a include BC, POM, sulfur dioxide, nitrogen oxides, carbon  
168 monoxide, volatile organic compounds, and ammonium, with their annual global budgets for the  
169 year 2010 shown in Table 1. ECLIPSE V5a emissions available at 0.5° latitude by 0.5° longitude  
170 spatial resolutions are re-gridded to the model spatial resolution. ECLIPSE V5a does not include  
171 shipping or wildfire biomass burning emissions, which are instead obtained from the IPCC AR5  
172 RCP8.5 scenario for the year 2010 (Riahi et al., 2011).

## 173 **2.4 Simulations: BC not active as IN**

174 Atmosphere-only simulations are performed in specified dynamics (SD) mode with offline  
175 meteorological fields from the Goddard Earth Observing System model version 5 (GEOS-5). In  
176 this SD mode configuration, the internally derived meteorological fields (e.g., horizontal wind  
177 component, air temperature and latent heat flux) are nudged by 10% towards reanalysis fields from  
178 GEOS-5 for every model time step. The nudging technique in CAM5-Chem has been evaluated to  
179 quantify the aerosol indirect effect in order to reduce the influence of natural variability  
180 (Kooperman et al., 2012). Sea surface temperature and sea ice in the model are prescribed from  
181 the Climatological/Slab-Ocean Data Model (DOCN) and Climatological Ice Model (DICE)  
182 respectively, with monthly-varying decadal mean averaged over 1981-2010.

183 We perform three sets of model simulations using the model configurations shown in Table 2. The  
184 first set of simulations represents the control with anthropogenic emissions following ECLIPSE  
185 V5a, as described above (hereafter referred to as BASE). The second set of simulations are



186 identical to the BASE simulation except the global solid fuel cookstove emissions for aerosols and  
187 gas-phase aerosol and ozone precursors are set to zero (termed as GBLSF\_OFF). The third set of  
188 simulations is identical to BASE except the solid fuel cookstove emissions are set to zero over the  
189 Indian sub-continent (termed as INDSF\_OFF). We run all the above simulations for 6 years from  
190 2005 to 2010, with the first year discarded as spin-up and the last five years averaged for output  
191 analysis. The differences between BASE and GBLSF\_OFF isolate the impacts of the global solid  
192 fuel cookstove sector aerosol emissions, and the differences between BASE and INDSF\_OFF  
193 isolate the impacts of the Indian solid fuel cookstove sector aerosol emissions. Top-of-the-  
194 atmosphere (TOA) aerosol shortwave (SW) and longwave (LW) radiative effects are calculated  
195 using the Rapid Radiative Transfer Model for GCMs (RRTMG) that is coupled to CAM5-Chem  
196 (Ghan, 2013; Ghan et al., 2012).

## 197 **2.5 Simulations: BC active as IN**

198 In default CAM5-Chem, BC is not treated as IN (Liu et al., 2012; Tilmes et al., 2015). IN  
199 concentrations from homogeneous nucleation are calculated as a function of vertical velocity (Liu  
200 et al., 2007). Several lab and field studies indicate that BC particles can act as IN (Cozic et al.,  
201 2008; DeMott et al., 1999; Koehler et al., 2009; Kulkarni et al., 2016). Therefore, we conduct  
202 additional simulations that treat BC as an effective IN applying the ice nucleation scheme of  
203 Barahona and Nenes (2008, 2009). The scheme estimates maximum supersaturation and ice crystal  
204 concentrations and considers competition between homogeneous and heterogeneous freezing.  
205 Homogeneous nucleation occurs in solution droplets formed on soluble aerosols (mainly sulfate),  
206 while heterogeneous nucleation occurs on IN, which here are a small subset of mineral dust and  
207 black carbon particles. The heterogeneous freezing of BC and dust is described as a generalized  
208 ice nucleation spectrum.

209 We perform three additional model simulations, with model configurations identical to those in  
210 Table 2, except for the treatment of BC particles as effective IN. In addition, for each model  
211 simulation, we alter the plausible maximum freezing efficiency (MFE) of BC as 0.01, 0.05 and 0.1  
212 that provides an uncertainty range in the global climatic impact assessment.

## 213 **3 Results**

### 214 **3.1 Evaluation of surface BC and OA concentrations**

Surface observation networks from IMPROVE, EMEP, and various campaigns in China and India are employed to compare with model simulations, as shown in Figure 1. We diagnose the normalized mean bias (NMB) for each source region, calculated as

$$\text{NMB} = \left( \frac{\sum_i (M_i - O_i)}{\sum_i O_i} \right) \times 100\% \quad (1)$$

where M and O represent monthly mean model simulated and observational concentrations at site  $i$  respectively, and  $\sum$  is the sum over all the sites within a source region.

In general, the model simulated surface BC concentrations agree with observations to within a factor of 2, consistent with previous studies (Huang et al., 2013; Wang et al., 2011, 2014a, 2014b). A total of 41 surface BC observational sites are used to evaluate the model simulation over India (Fig. 1a). On average, the model underestimates surface BC concentrations by approximately 45% and 34% over urban and rural sites respectively, with a total NMB -41% (Fig. 1a), which implies a marked underestimation of the BC emissions in India. Previous modeling studies have also reported large underestimates of BC surface concentrations over India against observations (Gadhavi et al., 2015; He et al., 2014; Zhang et al., 2015). Part of the model/measurement discrepancy is related to a sampling bias because the majority of the observations are located over urban or heavily polluted regions. For China sites, the NMB value is -16% (Fig. 1b). Similar to India, the model substantially underestimates the surface BC concentrations over urban sites with a NMB of -30%. However, the model performs relatively well over rural areas, with a NMB close to zero. For IMPROVE, the NMB values for rural and urban sites are -15% and -43%, respectively, with a total NMB -28% (Fig. 1c). Over Europe, the model simulated surface BC concentrations agree quite well with observations, with a NMB value of -8%, although two urban sites show substantial model underestimation (Fig. 1d).

The 40 AMS surface OA measurements are grouped into three categories: East Asia (8 sites), North America (17 sites) and Europe (15 sites) (Spracklen et al., 2011a; Zhang et al., 2007; Zheng et al., 2015). Figure 2 shows the evaluation of simulated surface OA against observations. Over East Asia, the model slightly underestimates observed OA, with a NMB of  $-8.5 \pm 5\%$  (Fig. 2a). In contrast, the simulated OA concentrations overestimate the measurements by over a factor of 2 in North America, with a NMB value of  $124 \pm 24\%$  (Fig. 2b). For the European sites, we find a

simulated OA overestimation of measured concentrations by up to  $0.9 \pm 0.7 \mu\text{g m}^{-3}$ , corresponding to a NMB of  $+32 \pm 26\%$  (Fig. 2c).

### 3.2 Evaluation of model AOD

Figure 3 compares simulated AOD values against observations over nine regions across the globe, including India, China, Rest of Asia (excluding China and India), Africa, South America, North America, Europe, Australia and remote regions. Over India, the simulated annual mean AOD is lower than observations by about  $16 \pm 3\%$  (Fig. 3a), with large bias sources mainly from the northern India regions (e.g., New Delhi and Kanpur). This is consistent with Quennehen et al. (2016) who also reported that model simulated AOD values were generally lower than satellite-derived AOD over northern India, using the same emission inventory as our study. As discussed in Sect. 3.1, model simulated surface BC concentrations over India are also underestimated (by up to 41%), therefore, the low bias of model simulated AOD can be attributed, in part, to the underestimation of Indian BC emissions from ECLIPSE V5a emission inventory (Stohl et al., 2015), although global anthropogenic BC budgets in ECLIPSE V5a lie in the high end compared with previous studies (Bond et al., 2004, 2013; Janssens-Maenhout et al., 2015). The model underestimate of AOD from AERONET in India may also be related to the fairly coarse global model resolution, as previously reported by Pan et al. (2015) and Zhang et al. (2015). A similar pattern is found over China (Fig. 3b) and the rest of Asia (Fig. 3c), with NMB values of  $-21 \pm 4\%$  and  $-15 \pm 6\%$  respectively. Model simulated AOD values from several sites in West Asia (Fig. 3c) are higher than observations, which is probably caused by the model overestimation of dust emissions (He and Zhang, 2014). This directly leads to annual mean model simulated AOD values over Africa  $25 \pm 11\%$  higher than observations because Saharan dust emissions dominate the AOD over North Africa (Fig. 3d). For South America, the model generally agrees quite well with observations (Fig. 3e), except for a few sites where model simulated AOD values are lower than observations by more than a factor of 2. This is probably due to the model underestimation of biomass burning emissions there (Reddington et al., 2016). AOD values over North America (Fig. 3f) and Europe (Fig. 3g) are relatively lower (with values generally  $< 0.3$ ), due to lower anthropogenic emissions. In these two regions, modeled AOD agrees with observations within a factor of 2, with NMB values  $-20 \pm 4\%$  and  $-18 \pm 9\%$  respectively. CAM5-Chem overestimates AOD over Australia (Fig. 3h) and remote sites (Fig. 3i), with NMB values of  $+69 \pm 17\%$  and  $+47$

273  $\pm 12\%$ , respectively. Globally, model simulated AOD agrees quite well with observations, with  
274 NMB values close to zero.

### 275 3.3 Contribution of solid fuel cookstove sector emissions to atmospheric BC and POM

#### 276 3.3.1 BC

277 Annual BC emissions and budgets are reported in Table 3 based on the anthropogenic inventory  
278 from ECLIPSE V5a. Annual BC emissions from the global and Indian solid fuel cookstove  
279 emissions are 2.31 and 0.36 Tg yr<sup>-1</sup>, accounting for 23.7% and 3.7% of the total BC emissions. For  
280 the control simulation, global annual mean BC burden and lifetime are  $0.12 \pm 0.001$  Tg and  $4.5 \pm$   
281  $0.04$  days, respectively (Table 3), at the low end of the range estimated by AeroCom (Schulz et  
282 al., 2006; Textor et al., 2006).

283 Figure 4 shows the zonal mean BC concentrations from the control simulation (Fig. 4a), global  
284 (Fig. 4b) and Indian (Fig. 4c) solid fuel cookstove emissions respectively. For the control  
285 simulation, in general, the highest BC concentrations (by up to 0.40  $\mu\text{g m}^{-3}$ ) occur at the surface  
286 over the emission source regions in the mid-latitudes (e.g., China and India). In the tropics and  
287 mid-latitudes, zonal mean BC concentrations decrease with increasing altitude, due to wet removal  
288 and deposition, as found in Huang et al. (2013). A similar vertical distribution is observed for the  
289 impacts from global and Indian solid fuel cookstove emissions, although the magnitude is smaller,  
290 compared with the control simulation. Annual mean BC burdens from global and Indian solid fuel  
291 cookstove emissions account for about  $24.2 \pm 0.7\%$  and  $5.0 \pm 0.0\%$  of that in the control simulation  
292 ( $0.12 \pm 0.001$  Tg).

#### 293 3.3.2 POM

294 Global POM emissions are mainly from biomass burning (31 Tg yr<sup>-1</sup>) and anthropogenic emissions  
295 (18.9 Tg yr<sup>-1</sup>), with global and Indian solid fuel cookstove emissions accounting for, 21% and  
296 3.4% respectively, of the total POM emissions (Table 3). In our control simulation, the annual  
297 mean POM burden is  $0.66 \pm 0.006$  Tg, and the global annual mean POM lifetime is  $4.8 \pm 0.04$   
298 days (Table 3).

299 In Figure 5, we show the annual zonal mean POM concentrations for the control simulation (Fig.  
 300 5a) and for global (Fig. 5b) and Indian (Fig. 5c) solid fuel cookstove emissions. There are two  
 301 maxima in the annual zonal mean POM concentrations near the surface. One is located in the  
 302 tropics due to the large biomass burning emissions there, and the other is located over mid-latitude  
 303 regions and originates mainly from anthropogenic emissions (Chung and Seinfeld, 2002; Huang  
 304 et al., 2013). For POM concentrations from global solid fuel cookstove emissions, a single  
 305 maximum is evident in the Northern Hemisphere (NH) subtropics at the surface (Fig. 5b). The  
 306 surface maximum for the Indian solid fuel cookstove emissions reaches a maximum in the NH  
 307 subtropics. The annual mean POM burdens from global and Indian solid fuel cookstove emissions  
 308 are  $0.13 \pm 0.004$  Tg and  $0.027 \pm 0.002$  Tg respectively.

### 309 **3.4 Impacts of solid fuel cookstove aerosol emissions on global climate change**

#### 310 **3.4.1 Direct radiative effect (DRE)**

312 The DRE impacts of the global and Indian solid fuel cookstove emissions are shown in Figure 6.  
 313 For the global solid fuel cookstove sector, the globally averaged DRE from aerosol emissions is  
 314  $+70 \pm 3$  mW m<sup>-2</sup> without treating BC as IN, which is a warming effect. The positive DRE from  
 315 global solid fuel cookstove emissions shows large spatial variability, with the largest impacts  
 316 located over western Africa, followed by India and China (figure not shown). The contributions of  
 317 BC and POM to DRE are  $+105 \pm 4$  (warming) and  $-14 \pm 1$  (cooling) mW m<sup>-2</sup>, respectively. In other  
 318 words, the warming effect of BC is partially offset by the cooling effect from POM. Additional  
 319 cooling effects may come from sulfate and SOA. CAM5-Chem assumes that BC is internally  
 320 mixed with other components in the accumulation mode and simulates enhanced absorption (BC  
 321 mass absorption cross section =  $14.6 \text{ m}^2 \text{ g}^{-1}$ ) when BC is coated by soluble aerosol components  
 322 and water vapor (Ghan et al., 2012), which results in larger estimates of the DRE than for BC alone  
 323 (Bond et al., 2013; Jacobson, 2001b).

324 The DRE from Indian solid fuel cookstove emissions also corresponds to a net warming effect  
 325 (Fig. 6), with a global annual mean value of  $+11 \pm 1$  mW m<sup>-2</sup>. Large impacts are found over  
 326 continental India, the Tibetan Plateau and southeastern China. On a global annual basis, DRE  
 327 values from BC and POM emissions from the Indian solid fuel cookstove sector are  $+18 \pm 1$  and -  
 328  $3 \pm 0.2$  mW m<sup>-2</sup>, respectively.

Deleted: from

### 330 3.4.2 Aerosol indirect, semi-direct and surface albedo effects: BC not active as IN

331 Global annual mean AIE and SAE values from global and Indian solid fuel cookstove aerosol  
332 emissions are shown in Figure 6. In our study, AIE includes the first (albedo) and second (lifetime)  
333 indirect effects, as well as the semi-direct effect. Annually averaged AIE from the global solid fuel  
334 cookstove sector is  $-226 \pm 5 \text{ mW m}^{-2}$  (Fig. 6), with annual mean shortwave (SW) AIE  $-122 \pm 22$   
335  $\text{mW m}^{-2}$  and longwave (LW) AIE  $-104 \pm 17 \text{ mW m}^{-2}$ , without treating BC as IN. Both the annual  
336 mean SW and LW AIE thus yield cooling effects. The cooling signals of SW AIE mainly occur  
337 over the western coast of South America, west and east coasts of Africa, South China and Himalaya  
338 regions (figure not shown). This is directly linked to the contribution of global solid fuel cookstove  
339 aerosol emissions to CCN (Pierce et al., 2007), which increases the cloud droplet number  
340 concentrations (CDNC) and cloud liquid water path (CLWP). Figure 7 shows the global vertically-  
341 integrated distribution of CLWP from the contribution of global solid fuel cookstove aerosol  
342 emissions. The higher CLWP is due to the enhanced lifetime of liquid and mixed-phase clouds,  
343 which therefore reflect more solar radiation, leading to cooling effect. For the LW AIE, the largest  
344 cooling effect is found over tropical regions, especially over southern India and the Indian Ocean.  
345 In order to investigate the causes of the LW AIE cooling effect, we analyze the cloud fraction  
346 change over a defined region (Latitude:0-20°N; Longitude:60-90°E) due to the effect from the  
347 global solid fuel cookstove sector. As shown in Figure 8a, cloud fraction in the lower troposphere  
348 increases. However, in the middle and upper troposphere cloud fraction decreases by up to 0.6%,  
349 with the strongest decrease found at ~150 hPa. We further analyze the changes in shallow and deep  
350 convective mass fluxes of moisture over the same domain. As shown in Figure 8b, moist shallow  
351 convective mass flux generally shows increases in the lower troposphere, which means that solid  
352 fuel cookstove aerosol emissions enhance the convective transport of water vapor within the  
353 boundary layer. By contrast, the deep convective mass flux demonstrates decreases from surface  
354 up to the middle troposphere (Fig. 8c). This indicates that solid fuel cookstove aerosol emissions  
355 may stabilize the boundary layer and inhibit the transport of water vapor from the surface to the  
356 upper troposphere/lower stratosphere, which leads to decreases in ice cloud formation, thus  
357 reducing cloud cover in the upper troposphere and lower stratosphere (UTLS) region at around  
358 200 hPa (Fig. 8a) and a LW AIE cooling effect.

359 The global annual mean AIE from Indian solid fuel cookstove aerosol emissions accounts for  
 360 approximately 10% ( $-22 \pm 3 \text{ mW m}^{-2}$ ) relative to the value of AIE from the global solid fuel  
 361 cookstove sector (Fig. 6), with globally averaged SW and LW AIE values of  $-3 \pm 11$  and  $-19 \pm 11$   
 362  $\text{mW m}^{-2}$  respectively.

363 Global annual mean SAE values from global and Indian solid fuel cookstove sector are relatively  
 364 small:  $+15 \pm 3$  and  $-2 \pm 3 \text{ mW m}^{-2}$ , respectively (Fig. 6). The warming effect is mainly due to the  
 365 deposition of BC on the surface of snow and sea ice (Flanner et al., 2007; Ghan, 2013; Ghan et al.,  
 366 2012).

#### 367 3.4.3 Total radiative effect: BC not active as IN

368 The net total radiative effect of global and Indian solid fuel cookstove aerosol emissions are both  
 369 cooling, with the global annual mean estimated to be  $-141 \pm 4$  and  $-12 \pm 4 \text{ mW m}^{-2}$  respectively  
 370 (Fig. 6). This suggests that if we remove solid fuel cookstove aerosol emissions, it will result in  
 371 warming and thus slightly increased global surface air temperature. That being said, this is likely  
 372 to be quite sensitive to model representation of aerosol mixing state (Fierce et al., 2017).

#### 373 3.4.4 Total radiative effect: BC active as IN

374 For the radiative effect of global solid fuel cookstove emissions with BC as IN, global annual mean  
 375 DRE is  $105 \pm 13 \text{ mW m}^{-2}$ , ranging from +90 to  $+115 \text{ mW m}^{-2}$ , which is 29-64% higher than the  
 376 DRE values from the default scheme (Fig. 6). Intriguingly, large globally averaged negative SW  
 377 AIE ( $-1.36 \pm 0.63 \text{ W m}^{-2}$ ) and positive LW AIE ( $+1.18 \pm 0.44 \text{ W m}^{-2}$ ) for global solid fuel  
 378 cookstove aerosol emissions are found, with annual mean values for the SW AIE ranging from -  
 379 1.83 to  $-0.64 \text{ W m}^{-2}$  and from +0.67 to  $+1.45 \text{ W m}^{-2}$  for the LW AIE. This results in a rather  
 380 uncertain net AIE, with a global annual mean AIE of  $-177 \pm 223 \text{ mW m}^{-2}$  (Fig. 6). The reason for  
 381 the large global annual average negative SW AIE and positive LW AIE is a substantial increase in  
 382 high cloud ( $< 500 \text{ hPa}$ ) fractions when BC acts as an efficient IN. For instance, with MFE = 0.1,  
 383 large increases (by up to 9%) in high cloud fractions from global solid fuel cookstove aerosol  
 384 emissions are found over subtropical regions, especially over the southern Atlantic Ocean (Fig. 9).  
 385 With BC particles active as IN, ice particle sizes become smaller, leading to a slower settling  
 386 velocity for ice particles and thus an increase in the lifetime of ice clouds. Increases in high clouds

**Deleted:** In default CAM5-Chem, BC is not treated as IN (Liu et al., 2012; Tilmes et al., 2015). However, several lab and field studies have shown that BC particles could act as IN (Cozic et al., 2008; DeMott et al., 1999; Koehler et al., 2009; Kulkarni et al., 2016), as discussed in Section 1. Therefore, we conduct sensitivity studies in our model simulations by treating BC as an effective IN, with the ice nucleation scheme by Barahona and Nenes (2008, 2009). We run three additional model simulations, with model configurations identical to those in Table 2, except for the treatment of BC particles as effective IN. In addition, for each model simulation, we alter the plausible maximum freezing efficiency (MFE) of BC as 0.01, 0.05 and 0.1, from which the uncertainty ranges of the climatic impacts from global and Indian solid fuel cookstove aerosol emissions with BC as IN are quantified.

not only reflect more solar radiation back to space, but also trap more LW radiation within the troposphere. For SAE, the global annual mean value is  $+12 \pm 10 \text{ mW m}^{-2}$  (Fig. 6). As a result, the net total radiative effect of global solid fuel cookstove aerosol emissions ranges from -275 to +154  $\text{mW m}^{-2}$ , with a global annual mean of  $-59 \pm 215 \text{ mW m}^{-2}$  (Fig. 6). Again, the source of the large uncertainty of the total radiative effect is due to the choice of MFE values. With  $\text{MFE} = 0.01$ , the global mean LW AIE ( $+672 \text{ mW m}^{-2}$ ) outweighs SW AIE ( $-638 \text{ mW m}^{-2}$ ), and therefore results in a net warming effect. For other MFE values (0.05 and 0.1), the absolute global annual mean SW AIE values are always higher than the LW AIE, leading to a net negative (i.e., cooling) total radiative effect.

For the Indian solid fuel cookstove sector, the global annual mean net total radiative effect is  $0.3 \pm 29 \text{ mW m}^{-2}$ , with an AIE of  $-18 \pm 37$  and a SAE of  $+1 \pm 8 \text{ mW m}^{-2}$ , respectively.

#### 4 Discussion and Summary

In this study, we employ the atmospheric component of a global 3-D climate model CESM v1.2.2, CAM5.3-Chem, to investigate the impacts of solid fuel cookstove emissions on global climate change. We update the default anthropogenic emission inventory using IIASA ECLIPSE V5a for the year 2010. We focus our analysis on the radiative effects of global and Indian solid fuel cookstove aerosol emissions. Model performance is evaluated against a global dataset of BC and OA measurements from surface sites and AOD from AERONET. Compared with observations, the model successfully reproduces the spatial patterns of atmospheric BC and OA concentrations, and generally agrees with measurements to within a factor of 2. Globally, the simulated AOD agrees quite well with observations, with NMB values close to zero. Nevertheless, the model tends to underestimate AOD values over source regions (except for Africa) and overestimate AOD over remote regions. The underestimates of AOD over India and China indicate that anthropogenic emissions of carbonaceous aerosols and sulfate precursors in ECLIPSE V5a are underestimated because carbonaceous aerosols and sulfate account for over 60% of the AOD over these two countries (Lu et al., 2011; Streets et al., 2009), which may introduce uncertainties for our climate estimates. The simulations reflect a present-day climatology forced with recycled year 2010 anthropogenic emissions. Model simulated BC concentrations were sampled in exact correspondence to the observed temporal period. In some limited cases, OA and AOD are not



exactly temporally consistent with the available aerosol measurement network climatologies applied in the evaluation. For regions where carbonaceous aerosol emissions have undergone substantial changes over short periods in the past few years, the model-measurement comparison may therefore introduce additional uncertainty. However, we focus the evaluation on the large-scale regional aerosol system dynamics. In the control simulation, the global annual mean BC burden and lifetime are  $0.12 \pm 0.001$  Tg and  $4.5 \pm 0.04$  days. For POM, the burden and lifetime are  $0.66 \pm 0.006$  Tg and  $4.8 \pm 0.04$  days. Annual mean surface BC (POM) concentrations over Northern India, East China and sub-Saharan Africa are  $1.55 \pm 0.076$ ,  $0.76 \pm 0.028$  and  $0.11 \pm 0.004$   $\mu\text{g m}^{-3}$  ( $7.11 \pm 0.32$ ,  $3.95 \pm 0.12$  and  $0.48 \pm 0.02$   $\mu\text{g m}^{-3}$ ), respectively. BC and POM burdens from global solid fuel cookstove emissions are  $0.029 \pm 0.001$  and  $0.13 \pm 0.004$  Tg, while contributions from the Indian sector are  $0.006 \pm 0.000$  and  $0.027 \pm 0.004$  Tg, respectively.

In the default CESM simulations without treating BC as IN, globally averaged DRE values from global and Indian solid fuel cookstove emissions are  $+70 \pm 3$  and  $+11 \pm 1$   $\text{mW m}^{-2}$ , respectively. The contributions of BC and POM from global solid fuel cookstove emissions to the DRE are  $+105 \pm 4$  and  $-14 \pm 1$   $\text{mW m}^{-2}$ . Global annual mean SW and LW AIE values from global solid fuel cookstove emissions are  $-122 \pm 22$  and  $-104 \pm 17$   $\text{mW m}^{-2}$ , with contributions from India yielding  $-3 \pm 11$   $\text{mW m}^{-2}$  for the SW AIE and  $-19 \pm 11$   $\text{mW m}^{-2}$  for the LW AIE, respectively. The cooling effect of the SW AIE is associated with the increases of CCN and CDNC, whereas the negative effects of LW AIE are caused by the suppression of convection that transports water vapor from lower troposphere to upper troposphere/stratosphere, thus reducing ice cloud cover. The CAM5-Chem also computes the SAE, with global and Indian solid fuel cookstove emissions contributing  $+15 \pm 3$  and  $-2 \pm 3$   $\text{mW m}^{-2}$ , respectively. As a result, the net total radiative effects of global and Indian solid fuel cookstove emissions are  $-141 \pm 4$  and  $-12 \pm 4$   $\text{mW m}^{-2}$ , respectively, both producing a net cooling effect.

Sensitivity studies are carried out to examine the impacts of global and Indian solid fuel cookstove emissions on climate by treating BC as an effective IN, with MFE as 0.01, 0.05 and 0.1, respectively. For the climate impacts of global solid fuel cookstove emissions, global annual mean DRE is  $+105 \pm 13$   $\text{mW m}^{-2}$ , which is  $\sim 50\%$  higher than the default model scheme in which BC particles are not treated as IN (Fig. 6). This is driven by the increases of BC burden (due to prolonged BC lifetimes) from global solid fuel cookstove emissions by up to 17% with BC as IN.

462 Because the BC absorption effect dominates the DRE, increases in BC burden enhance the  
 463 magnitude of annual mean DRE (Jacobson, 2001a). Compared with the default model scheme,  
 464 significant changes in globally averaged SW AIE are found, with a global annual mean of  $-1.36 \pm$   
 465  $0.63 \text{ W m}^{-2}$ , which is about an order of magnitude higher than that from the default scheme.  
 466 Moreover, in contrast to the cooling effect found in the default scheme, annual mean positive LW  
 467 AIE is simulated here ( $+1.18 \pm 0.44 \text{ W m}^{-2}$ ). The above changes in cookstove emission induced  
 468 SW and LW AIE are caused by the substantial increases in high cloud ( $< 500 \text{ hPa}$ ) fractions with  
 469 BC particles acting as IN by up to 9% due to the effect of solid fuel cookstove emissions. Large  
 470 increases in high cloud fractions are found mainly over tropical regions, especially over southern  
 471 Africa. For the SAE, similar to the model default scheme, the global annual mean value is  $+12 \pm$   
 472  $10 \text{ mW m}^{-2}$ . Summing up the DRE, the AIE and the SAE, the net total radiative effect of global  
 473 solid fuel cookstove emissions is  $-59 \pm 215 \text{ mW m}^{-2}$ . For the Indian sector, the global mean total  
 474 radiative effect is  $0.3 \pm 29 \text{ mW m}^{-2}$ , with a net AIE  $-18 \pm 37$  and a SAE  $+1 \pm 8 \text{ mW m}^{-2}$ ,  
 475 respectively.

476 We compare our simulation results with previous studies as shown in Figure 10. The globally  
 477 averaged DRE in our control simulation is more than four times higher than that from the baseline  
 478 simulation of Kodros et al. (2015), which assumes homogeneous particle mixing state (Fig. 10).  
 479 Annual emissions of BC from global solid fuel cookstove sector in our study ( $2.3 \text{ Tg C yr}^{-1}$ ) is  
 480 approximately 44% higher than that from global biofuel emissions ( $1.6 \text{ Tg C yr}^{-1}$ ) in Kodros et al.  
 481 (2015), which, to some extent, leads to differences in annual mean DRE values together with  
 482 different optical calculations. The annual mean DRE value from another study by Butt et al. (2016)  
 483 differs from ours in magnitude and sign, and concluded that annually averaged DRE from  
 484 residential combustion sources was  $-5 \text{ mW m}^{-2}$  (Fig. 10). The negative effect of DRE in Butt et al.  
 485 (2016) is partially driven by the inclusion of  $\text{SO}_2$  emissions ( $8.9 \text{ Tg SO}_2 \text{ yr}^{-1}$ ) from commercial  
 486 coal combustion in the residential sector, leading to the cooling effect of sulfate and organic  
 487 aerosols outweighing the warming from BC. For AIE, our control simulation is 38 times higher  
 488 than that from Kodros et al. (2015) and over an order of magnitude higher than that from Butt et  
 489 al. (2016). Consistent with our study, Ward et al. (2012) also found a large AIE ( $-1.74$  to  $1.00 \text{ W}$   
 490  $\text{m}^{-2}$ ) for carbonaceous aerosols from fires using CESM CAM4-Chem. Both Kodros et al. (2015)  
 491 and Butt et al. (2016) used offline radiative models to calculate AIE and only considered the first  
 492 (albedo) aerosol indirect effect, which may partially explain the AIE differences. As mentioned

earlier, the AIE in our study includes aerosol first and second indirect effects as well as the semi-direct effect. Lacey and Henze (2015) estimated that the global surface air temperature changes due to solid wood fuel removal ranged from -0.28 K (cooling) to +0.16 K (warming), with a central estimate of -0.06 K (cooling). This cooling estimate is opposite to our study. However, we acknowledge that there are fundamental differences in calculating the radiative effect between our study and Lacey and Henze (2015), which employed absolute regional temperature potentials to quantify the climate responses.

Cookstove intervention programs have been implemented in developing countries, such as China, India and some African countries, to improve air quality and human health and to mitigate climate change (Anenberg et al., 2017; Aung et al., 2016; Carter et al., 2016). Our results suggest that large-scale efforts to replace inefficient cookstoves in developing countries with advanced technologies is not likely to reduce global warming through aerosol reductions, and may even lead to increased global warming when aerosol-cloud interactions are taken into account. Therefore, without improved constraints on BC interactions with clouds, especially mixed-phase and ice clouds, the net sign of the impacts of carbonaceous aerosols from solid fuel cookstoves on global climate (warming or cooling) remains ambiguous. This study does not include the greenhouse gas emission effects from the solid fuel cookstove sector, which may indeed be large enough to imply a net warming global climate impact depending on time scale. (Lacey et al., 2017).

## Acknowledgements

This article was developed under Assistance Agreement No. R835421 awarded by the U.S. Environmental Protection Agency to SEI. It has not been formally reviewed by EPA. The views expressed in this document are solely those of the authors and do not necessarily reflect those of the Agency. EPA does not endorse any products or commercial services mentioned in this publication. N. Unger acknowledges support from the University of Exeter, UK. We are thankful for helpful discussions with S. Tilmes and S. Ghan. This project was supported in part by the facilities and staff of the Yale University High Performance Computing Center.

## References

Amann, M., Bertok, I., Borken-Kleefeld, J., Cofala, J., Heyes, C., Höglund-Isaksson, L.,

521 Klimont, Z., Nguyen, B., Posch, M., Rafaj, P., Sandler, R., Schöpp, W., Wagner, F. and  
 522 Winiwarter, W.: Cost-effective control of air quality and greenhouse gases in Europe: Modeling  
 523 and policy applications, *Environ. Model. Softw.*, 26(12), 1489–1501,  
 524 doi:10.1016/j.envsoft.2011.07.012, 2011.

525 Amann, M., Klimont, Z. and Wagner, F.: Regional and Global Emissions of Air Pollutants:  
 526 Recent Trends and Future Scenarios, *Annu. Rev. Environ. Resour.*, 38(1), 31–55,  
 527 doi:10.1146/annurev-environ-052912-173303, 2013.

528 Anenberg, S. C., Henze, D. K., Lacey, F., Irfan, A., Kinney, P., Kleiman, G. and Pillarisetti, A.:  
 529 Air pollution-related health and climate benefits of clean cookstove programs in Mozambique,  
 530 *Environ. Res. Lett.*, 12(2), 25006, doi:10.1088/1748-9326/aa5557, 2017.

531 Archer-Nicholls, S., Carter, E., Kumar, R., Xiao, Q., Liu, Y., Frostad, J., Forouzanfar, M. H.,  
 532 Cohen, A., Brauer, M., Baumgartner, J. and Wiedinmyer, C.: The regional impacts of cooking  
 533 and heating emissions on ambient air quality and disease burden in China, *Environ. Sci.*  
 534 *Technol.*, 50(17), 9416–9423, doi:10.1021/acs.est.6b02533, 2016.

535 Aung, T. W., Jain, G., Sethuraman, K., Baumgartner, J., Reynolds, C., Grieshop, A. P., Marshall,  
 536 J. D. and Brauer, M.: Health and Climate-Relevant Pollutant Concentrations from a Carbon-  
 537 Finance Approved Cookstove Intervention in Rural India, *Environ. Sci. Technol.*, 50(13), 7228–  
 538 7238, doi:10.1021/acs.est.5b06208, 2016.

539 Barahona, D. and Nenes, A.: Parameterization of cirrus cloud formation in large-scale models:  
 540 Homogeneous nucleation, *J. Geophys. Res. Atmos.*, 113(11), 1–15, doi:10.1029/2007JD009355,  
 541 2008.

542 Barahona, D. and Nenes, A.: Parameterizing the competition between homogeneous and  
 543 heterogeneous freezing in ice cloud formation – polydisperse ice nuclei, *Atmos. Chem. Phys.*, 9,  
 544 5933–5948, doi:10.5194/acp-9-5933-2009, 2009.

545 Bauer, S. E., Menon, S., Koch, D., Bond, T. C. and Tsigaridis, K.: A global modeling study on  
 546 carbonaceous aerosol microphysical characteristics and radiative effects, *Atmos. Chem. Phys.*,  
 547 10(15), 7439–7456, doi:10.5194/acp-10-7439-2010, 2010.

548 Bond, T., Venkataraman, C. and Masera, O.: Global atmospheric impacts of residential fuels,  
549 *Energy Sustain. Dev.*, 8(3), 20–32, doi:10.1016/S0973-0826(08)60464-0, 2004.

550 Bond, T. C., Doherty, S. J., Fahey, D. W., Forster, P. M., Berntsen, T., Deangelo, B. J., Flanner,  
551 M. G., Ghan, S., Kärcher, B., Koch, D., Kinne, S., Kondo, Y., Quinn, P. K., Sarofim, M. C.,  
552 Schultz, M. G., Schulz, M., Venkataraman, C., Zhang, H., Zhang, S., Bellouin, N., Guttikunda,  
553 S. K., Hopke, P. K., Jacobson, M. Z., Kaiser, J. W., Klimont, Z., Lohmann, U., Schwarz, J. P.,  
554 Shindell, D., Storelvmo, T., Warren, S. G. and Zender, C. S.: Bounding the role of black carbon  
555 in the climate system: A scientific assessment, *J. Geophys. Res. Atmos.*, 118(11), 5380–5552,  
556 doi:10.1002/jgrd.50171, 2013.

557 Bonjour, S., Wolf, J. and Lahiff, M.: Solid Fuel Use for Household Cooking: Country and  
558 Regional Estimates for 1980–2010, *Environ. Health Perspect.*, 121(7), 784–790,  
559 doi:10.1289/ehp.1205987, 2013.

560 Boucher, O., Randall, D., Artaxo, P., Bretherton, C., Feingold, G., Forster, P., Kerminen, V.-M.  
561 V.-M., Kondo, Y., Liao, H., Lohmann, U., Rasch, P., Satheesh, S. K., Sherwood, S., Stevens, B.,  
562 Zhang, X. Y. and Zhan, X. Y.: Clouds and Aerosols, *Clim. Chang.* 2013 *Phys. Sci. Basis*.  
563 *Contrib. Work. Gr. I to Fifth Assess. Rep. Intergov. Panel Clim. Chang.*, 571–657,  
564 doi:10.1017/CBO9781107415324.016, 2013.

565 Butt, E. W., Rap, A., Schmidt, A., Scott, C. E., Pringle, K. J., Reddington, C. L., Richards, N. A.  
566 D., Woodhouse, M. T., Ramirez-Villegas, J., Yang, H., Vakkari, V., Stone, E. A., Rupakheti, M.,  
567 Praveen, P. S., Van Zyl, P. G., Beukes, J. P., Josipovic, M., Mitchell, E. J. S., Sallu, S. M.,  
568 Forster, P. M. and Spracklen, D. V.: The impact of residential combustion emissions on  
569 atmospheric aerosol, human health, and climate, *Atmos. Chem. Phys.*, 16(2), 873–905,  
570 doi:10.5194/acp-16-873-2016, 2016.

571 Carter, E., Archer-Nicholls, S., Ni, K., Lai, A. M., Niu, H., Secrest, M. H., Sauer, S. M., Schauer,  
572 J. J., Ezzati, M., Wiedinmyer, C., Yang, X. and Baumgartner, J.: Seasonal and Diurnal Air  
573 Pollution from Residential Cooking and Space Heating in the Eastern Tibetan Plateau, *Environ.*  
574 *Sci. Technol.*, 50(15), 8353–8361, doi:10.1021/acs.est.6b00082, 2016.

575 Chow, J. C., Watson, J. G., Pritchett, L. C., Pierson, W. R., Frazer, C. A. and Purcell, R. G.: THE

576 DRI THERMAL/OPTICAL REFLECTANCE CARBON ANALYSIS SYSTEM :  
577 DESCRIPTION, EVALUATION AND APPLICATIONS IN U.S. AIR QUALITY STUDIES,  
578 Atmos. Environ., 27A(8), 1185–1201, 1993.

579 Chow, J. C., Watson, J. G., Chen, L.-W. A., Arnott, W. P. and Moosmuller, H.: Equivalence of  
580 Elemental Carbon by Thermal/Optical Reflectance and Transmittance with Different  
581 Temperature Protocols, Environ. Sci. Technol., 38(16), 4414–4422, 2004.

582 Chung, S. H.: Climate response of direct radiative forcing of anthropogenic black carbon, J.  
583 Geophys. Res., 110(D11), D11102, doi:10.1029/2004JD005441, 2005.

584 Chung, S. H. and Seinfeld, J. H.: Global distribution and climate forcing of carbonaceous  
585 aerosols, J. Geophys. Res. Atmos., 107(19), doi:10.1029/2001JD001397, 2002.

586 Chylek, P. and Wong, J.: Effect of absorbing aerosols on global radiation budget, Geophys. Res.  
587 Lett., 22(8), 929–931, 1995.

588 Cozic, J., Mertes, S., Verheggen, B., Cziczo, D. J., Gallavardin, S. J., Walter, S., Baltensperger,  
589 U. and Weingartner, E.: Black carbon enrichment in atmospheric ice particle residuals observed  
590 in lower tropospheric mixed phase clouds, J. Geophys. Res. Atmos., 113(15), 1–11,  
591 doi:10.1029/2007JD009266, 2008.

592 DeMott, P. J., Chen, Y., Kreidenweis, S. M., Rogers, D. C. and Sherman, D. E.: Ice formation by  
593 black carbon particles, Geophys. Res. Lett., 26(16), 2429–2432, doi:10.1029/1999GL900580,  
594 1999.

595 Dubovikl, O. and King, M. D.: A flexible inversion algorithm for retrieval of aerosol optical  
596 properties from Sun and sky radiance measurements, J. Geophys. Res., 105696(27), 673–20,  
597 doi:10.1029/2000JD900282, 2000.

598 EMEP/MS-CW, EMEP/CCC, EMEP/CEIP, IDAEA-CSIC, CCE/RIVM and FMI:  
599 Transboundary particulate matter, photo-oxidants, acidifying and eutrophying components.,  
600 2014.

601 Emmons, L. K., Walters, S., Hess, P. G., Lamarque, J.-F., Pfister, G. G., Fillmore, D., Granier,

602 C., Guenther, A., Kinnison, D., Laepple, T., Orlando, J., Tie, X., Tyndall, G., Wiedinmyer, C.,  
603 Baughcum, S. L. and Kloster, S.: Description and evaluation of the Model for Ozone and Related  
604 chemical Tracers, version 4 (MOZART-4), *Geosci. Model Dev.*, 3, 43–67, doi:10.5194/gmd-3-  
605 43-2010, 2010.

606 Ezzati, M. and Kammen, D. M.: The health impacts of exposure to indoor air pollution from  
607 solid fuels in developing countries: Knowledge, gaps, and data needs, *Environ. Health Perspect.*,  
608 110(11), 1057–1068, doi:10.1289/ehp.021101057, 2002.

609 Fierce, L., Riemer, N. and Bond, T. C.: Toward reduced representation of mixing state for  
610 simulating aerosol effects on climate, *Bull. Am. Meteorol. Soc.*, 98(5), 971–980,  
611 doi:10.1175/BAMS-D-16-0028.1, 2017.

612 Flanner, M. G., Zender, C. S., Randerson, J. T. and Rasch, P. J.: Present-day climate forcing and  
613 response from black carbon in snow, *J. Geophys. Res. Atmos.*, 112(11), 1–17,  
614 doi:10.1029/2006JD008003, 2007.

615 Gadhavi, H. S., Renuka, K., Ravi Kiran, V., Jayaraman, A., Stohl, A., Klimont, Z. and Beig, G.:  
616 Evaluation of black carbon emission inventories using a Lagrangian dispersion model - A case  
617 study over southern India, *Atmos. Chem. Phys.*, 15(3), 1447–1461, doi:10.5194/acp-15-1447-  
618 2015, 2015.

619 Garland, C., Delapena, S., Prasad, R., L'Orange, C., Alexander, D. and Johnson, M.: Black  
620 carbon cookstove emissions: A field assessment of 19 stove/fuel combinations, *Atmos. Environ.*,  
621 169, 140–149, doi:10.1016/j.atmosenv.2017.08.040, 2017.

622 GBD 2015 Risk Factors Collaborators: Global, regional, and national comparative risk  
623 assessment of 79 behavioural, environmental and occupational, and metabolic risks or clusters of  
624 risks, 1990–2015: a systematic analysis for the Global Burden of Disease Study 2015, *Lancet*,  
625 388(10053), 1659–1724, doi:10.1016/S0140-6736(16)31679-8, 2016.

626 Gettelman, A., Liu, X., Barahona, D., Lohmann, U. and Chen, C.: Climate impacts of ice  
627 nucleation, *J. Geophys. Res. Atmos.*, 117(20), 1–14, doi:10.1029/2012JD017950, 2012.

628 Ghan, S. J.: Technical note: Estimating aerosol effects on cloud radiative forcing, *Atmos. Chem.*

629 Phys., 13(19), 9971–9974, doi:10.5194/acp-13-9971-2013, 2013.

630 Ghan, S. J., Liu, X., Easter, R. C., Zaveri, R., Rasch, P. J., Yoon, J. H. and Eaton, B.: Toward a  
631 minimal representation of aerosols in climate models: Comparative decomposition of aerosol  
632 direct, semidirect, and indirect radiative forcing, *J. Clim.*, 25(19), 6461–6476, doi:10.1175/JCLI-  
633 D-11-00650.1, 2012.

634 Hanbar, R. D. and Karve, P.: National Programme on Improved Chulha (NPIC) of the  
635 Government of India: An overview, *Energy Sustain. Dev.*, 6(2), 49–55, doi:10.1016/S0973-  
636 0826(08)60313-0, 2002.

637 He, C., Li, Q. B., Liou, K. N., Zhang, J., Qi, L., Mao, Y., Gao, M., Lu, Z., Streets, D. G., Zhang,  
638 Q., Sarin, M. M. and Ram, K.: A global 3-D CTM evaluation of black carbon in the Tibetan  
639 Plateau, *Atmos. Chem. Phys.*, 14(13), 7091–7112, doi:10.5194/acp-14-7091-2014, 2014.

640 He, J. and Zhang, Y.: Improvement and further development in CESM/CAM5: Gas-phase  
641 chemistry and inorganic aerosol treatments, *Atmos. Chem. Phys.*, 14(17), 9171–9200,  
642 doi:10.5194/acp-14-9171-2014, 2014.

643 Holben, B. N., Eck, T. F., Slutsker, I., Tanré, D., Buis, J. P., Setzer, A., Vermote, E., Reagan, J.  
644 A., Kaufman, Y. J., Nakajima, T., Lavenue, F., Jankowiak, I. and Smirnov, A.: AERONET—A  
645 Federated Instrument Network and Data Archive for Aerosol Characterization, *Remote Sens.*  
646 *Environ.*, 66(1), 1–16, doi:10.1016/S0034-4257(98)00031-5, 1998.

647 Holben, B. N., Tanré, D., Smirnov, a., Eck, T. F., Slutsker, I., Abuhassan, N., Newcomb, W. W.,  
648 Schafer, J. S., Chatenet, B., Lavenue, F., Kaufman, Y. J., Castle, J. Vande, Setzer, a., Markham,  
649 B., Clark, D., Frouin, R., Halthore, R., Karneli, a., O’Neill, N. T., Pietras, C., Pinker, R. T.,  
650 Voss, K. and Zibordi, G.: An emerging ground-based aerosol climatology: Aerosol optical depth  
651 from AERONET, *J. Geophys. Res.*, 106(D11), 12067, doi:10.1029/2001JD900014, 2001.

652 Huang, Y., Wu, S., Dubey, M. K. and French, N. H. F.: Impact of aging mechanism on model  
653 simulated carbonaceous aerosols, *Atmos. Chem. Phys.*, 13(13), 6329–6343, doi:10.5194/acp-13-  
654 6329-2013, 2013.

655 Jacobson, M. Z.: Global direct radiative forcing due to multicomponent natural and anthropogenic



656 aerosols, *J. Geophys. Res.*, 106(D2), 1551–1568, doi:10.1029/2000JD900514, 2001a.

657 Jacobson, M. Z.: Strong radiative heating due to the mixing state of black carbon in atmospheric  
658 aerosols., *Nature*, 409(6821), 695–697, doi:10.1038/35055518, 2001b.

659 Janssens-Maenhout, G., Crippa, M., Guizzardi, D., Dentener, F., Muntean, M., Pouliot, G.,  
660 Keating, T., Zhang, Q., Kurokawa, J., Wankmüller, R., Denier van der Gon, H., Kuenen, J. J. P.,  
661 Klimont, Z., Frost, G., Darras, S., Koffi, B. and Li, M.: HTAP\_v2.2: a mosaic of regional and  
662 global emission grid maps for 2008 and 2010 to study hemispheric transport of air pollution,  
663 *Atmos. Chem. Phys.*, 15(19), 11411–11432, doi:10.5194/acp-15-11411-2015, 2015.

664 Kanagawa, M. and Nakata, T.: Analysis of the energy access improvement and its socio-  
665 economic impacts in rural areas of developing countries, *Ecol. Econ.*, 62(2), 319–329,  
666 doi:10.1016/j.ecolecon.2006.06.005, 2007.

667 Karcher, B. and Hendricks, J.: Physically based parameterization of cirrus cloud formation for  
668 use in global atmospheric models, *J. Geophys. Res.*, 111, D01205, doi:10.1029/2005JD006219,  
669 2006.

670 Kishore, V. V. N. and Ramana, P. V.: Improved cookstoves in rural India: How improved are  
671 they? A critique of the perceived benefits from the National Programme on Improved Chulhas  
672 (NPIC), *Energy*, 27(1), 47–63, doi:10.1016/S0360-5442(01)00056-1, 2002.

673 Klimont, Z., Cofala, J., Wei, W., Zhang, C., Wang, S., Kejun, J., Bhandari, P., Mathur, R.,  
674 Purohit, P., Rafaj, P., Chambers, A., Amann, M. and Hao, J.: Projections of SO<sub>2</sub>, NO<sub>x</sub> and  
675 carbonaceous aerosols emissions in Asia, *Tellus, Ser. B Chem. Phys. Meteorol.*, (61B), 602–617,  
676 doi:10.1111/j.1600-0889.2009.00428.x, 2009.

677 Klimont, Z., Kupiainen, K., Heyes, C., Purohit, P., Cofala, J., Rafaj, P., Borken-Kleefeld, J. and  
678 Schöpp, W.: Global anthropogenic emissions of particulate matter including black carbon,  
679 *Atmos. Chem. Phys.*, 17(14), 8681–8723, doi:10.5194/acp-17-8681-2017, 2017.

680 Kodros, J. K., Scott, C. E., Farina, S. C., Lee, Y. H., L'Orange, C., Volckens, J. and Pierce, J. R.:  
681 Uncertainties in global aerosols and climate effects due to biofuel emissions, *Atmos. Chem.*  
682 *Phys.*, 15(15), 8577–8596, doi:10.5194/acp-15-8577-2015, 2015.

683 Koehler, K. A., DeMott, P. J., Kreidenweis, S. M., Popovicheva, O. B., Petters, M. D., Carrico,  
 684 C. M., Kireeva, E. D., Khokhlova, T. D. and Shonija, N. K.: Cloud condensation nuclei and ice  
 685 nucleation activity of hydrophobic and hydrophilic soot particles, *Phys. Chem. Chem. Phys.*,  
 686 11(36), 7906–7920, doi:10.1039/b916865f, 2009.

687 Kooperman, G. J., Pritchard, M. S., Ghan, S. J., Wang, M., Somerville, R. C. J. and Russell, L.  
 688 M.: Constraining the influence of natural variability to improve estimates of global aerosol  
 689 indirect effects in a nudged version of the Community Atmosphere Model 5, *J. Geophys. Res.*  
 690 *Atmos.*, 117(23), 1–16, doi:10.1029/2012JD018588, 2012.

691 Kulkarni, G., China, S., Liu, S., Nandasiri, M., Sharma, N., Wilson, J., Aiken, A. C., Chand, D.,  
 692 Laskin, A., Mazzoleni, C., Pekour, M., Shilling, J., Shutthanandan, V., Zelenyuk, A. and Zaveri,  
 693 R. A.: Ice nucleation activity of diesel soot particles at cirrus relevant temperature conditions:  
 694 Effects of hydration, secondary organics coating, soot morphology, and coagulation, *Geophys.*  
 695 *Res. Lett.*, 43(7), 3580–3588, doi:10.1002/2016GL068707, 2016.

696 Lacey, F. and Henze, D.: Global climate impacts of country-level primary carbonaceous aerosol  
 697 from solid-fuel cookstove emissions, *Environ. Res. Lett.*, 10(11), 114003, doi:10.1088/1748-  
 698 9326/10/11/114003, 2015.

699 Lacey, F. G., Henze, D. K., Lee, C. J., van Donkelaar, A. and Martin, R. V.: Transient climate  
 700 and ambient health impacts due to national solid fuel cookstove emissions, *Proc. Natl. Acad.*  
 701 *Sci.*, 114(6), 1269–1274, doi:10.1073/pnas.1612430114, 2017.

702 Lamarque, J. F., Emmons, L. K., Hess, P. G., Kinnison, D. E., Tilmes, S., Vitt, F., Heald, C. L.,  
 703 Holland, E. A., Lauritzen, P. H., Neu, J., Orlando, J. J., Rasch, P. J. and Tyndall, G. K.: CAM-  
 704 chem: Description and evaluation of interactive atmospheric chemistry in the Community Earth  
 705 System Model, *Geosci. Model Dev.*, 5(2), 369–411, doi:10.5194/gmd-5-369-2012, 2012.

706 Legros, G., Havet, I., Bruce, N. and Bonjour, S.: The Energy Access Situation in Developing  
 707 Countries, WHO UNDP, 142 [online] Available from:  
 708 <http://scholar.google.com/scholar?hl=en&btnG=Search&q=intitle:THE+ENERGY+ACCESS+SITUATION+IN+DEVELOPING+COUNTRIES+A+Review+Focusing+on+the#0>, 2009.

710 Lelieveld, J., Evans, J. S., Fnais, M., Giannadaki, D. and Pozzer, A.: The contribution of outdoor  
 711 air pollution sources to premature mortality on a global scale, *Nature*, 525(7569), 367–371,  
 712 doi:10.1038/nature15371, 2015.

713 Liu, J., Mauzerall, D. L., Chen, Q., Zhang, Q., Song, Y., Peng, W., Klimont, Z., Qiu, X., Zhang,  
 714 S., Hu, M., Lin, W., Smith, K. R. and Zhu, T.: Air pollutant emissions from Chinese households:  
 715 A major and underappreciated ambient pollution source, *Proc. Natl. Acad. Sci.*, 113(28), 7756–  
 716 7761, doi:10.1073/pnas.1604537113, 2016.

717 Liu, X. and Penner, J. E.: Ice nucleation parameterization for global models, *Meteorol.*  
 718 *Zeitschrift*, 14(4), 499–514, doi:10.1127/0941-2948/2005/0059, 2005.

719 Liu, X., Penner, J. E., Ghan, S. J. and Wang, M.: Inclusion of ice microphysics in the NCAR  
 720 Community Atmospheric Model version 3 (CAM3), *J. Clim.*, 20(18), 4526–4547,  
 721 doi:10.1175/JCLI4264.1, 2007.

722 Liu, X., Easter, R. C., Ghan, S. J., Zaveri, R., Rasch, P., Shi, X., Lamarque, J. F., Gettelman, A.,  
 723 Morrison, H., Vitt, F., Conley, A., Park, S., Neale, R., Hannay, C., Ekman, A. M. L., Hess, P.,  
 724 Mahowald, N., Collins, W., Iacono, M. J., Bretherton, C. S., Flanner, M. G. and Mitchell, D.:  
 725 Toward a minimal representation of aerosols in climate models: Description and evaluation in  
 726 the Community Atmosphere Model CAM5, *Geosci. Model Dev.*, 5(3), 709–739,  
 727 doi:10.5194/gmd-5-709-2012, 2012.

728 Lohmann, U.: A glaciation indirect aerosol effect caused by soot aerosols, *Geophys. Res. Lett.*,  
 729 29(4), 1052, doi:10.1029/2001gl014357, 2002.

730 Lohmann, U., Feichter, J., Penner, J. and Leaitch, R.: Indirect effect of sulfate and carbonaceous  
 731 aerosols: A mechanistic treatment, *J. Geophys. Res. Atmos.*, 105(D10), 12193–12206,  
 732 doi:10.1029/1999JD901199, 2000.

733 Lu, Z., Zhang, Q. and Streets, D. G.: Sulfur dioxide and primary carbonaceous aerosol emissions  
 734 in China and India, 1996-2010, *Atmos. Chem. Phys.*, 11(18), 9839–9864, doi:10.5194/acp-11-  
 735 9839-2011, 2011.

736 Malm, W. C., Sisler, J. F., Huffman, D., Eldred, R. A. and Cahill, T. A.: Spatial and seasonal

737 trends in particle concentration and optical extinction in the United States, *J. Geophys. Res.*,  
 738 99(D1), 1347–1370, doi:10.1029/93JD02916, 1994.

739 Myhre, G., Samset, B. H., Schulz, M., Balkanski, Y., Bauer, S., Bernsten, T. K., Bian, H.,  
 740 Bellouin, N., Chin, M., Diehl, T., Easter, R. C., Feichter, J., Ghan, S. J., Hauglustaine, D.,  
 741 Iversen, T., Kinne, S., Kirkevåg, A., Lamarque, J. F., Lin, G., Liu, X., Lund, M. T., Luo, G., Ma,  
 742 X., Van Noije, T., Penner, J. E., Rasch, P. J., Ruiz, A., Seland, Skeie, R. B., Stier, P., Takemura,  
 743 T., Tsigaridis, K., Wang, P., Wang, Z., Xu, L., Yu, H., Yu, F., Yoon, J. H., Zhang, K., Zhang, H.  
 744 and Zhou, C.: Radiative forcing of the direct aerosol effect from AeroCom Phase II simulations,  
 745 *Atmos. Chem. Phys.*, 13(4), 1853–1877, doi:10.5194/acp-13-1853-2013, 2013.

746 Pan, X., Chin, M., Gautam, R., Bian, H., Kim, D., Colarco, P. R., Diehl, T. L., Takemura, T. and  
 747 Pozzoli, L.: A multi-model evaluation of aerosols over South Asia : common, , 5903–5928,  
 748 doi:10.5194/acp-15-5903-2015, 2015.

749 Penner, J. E., Dickinson, R. E. and O'Neill, C. A.: Effects of Aerosol from Biomass Burning on  
 750 the Global Radiation Budget, *Science*, 256(5062), 1432–1435,  
 751 doi:10.1126/science.256.5062.1432, 1992.

752 Penner, J. E., Chen, Y., Wang, M. and Liu, X.: Possible influence of anthropogenic aerosols on  
 753 cirrus clouds and anthropogenic forcing, *Atmos. Chem. Phys.*, 9(3), 879–896, doi:10.5194/acp-9-  
 754 879-2009, 2009.

755 Pierce, J. R., Chen, K. and Adams, P. J.: Contribution of carbonaceous aerosol to cloud  
 756 condensation nuclei: processes and uncertainties evaluated with a global aerosol microphysics  
 757 model, *Atmos. Chem. Phys.*, 7, 5447–5466, doi:10.5194/acp-7-5447-2007, 2007.

758 Quennehen, B., Raut, J. C., Law, K. S., Daskalakis, N., Ancellet, G., Clerbaux, C., Kim, S. W.,  
 759 Lund, M. T., Myhre, G., Olivié, D. J. L., Safieddine, S., Skeie, R. B., Thomas, J. L., Tsyro, S.,  
 760 Bazureau, A., Bellouin, N., Hu, M., Kanakidou, M., Klimont, Z., Kupiainen, K.,  
 761 Myriokefalitakis, S., Quaas, J., Rumbold, S. T., Schulz, M., Cherian, R., Shimizu, A., Wang, J.,  
 762 Yoon, S. C. and Zhu, T.: Multi-model evaluation of short-lived pollutant distributions over east  
 763 Asia during summer 2008, *Atmos. Chem. Phys.*, 16(17), 10765–10792, doi:10.5194/acp-16-  
 764 10765-2016, 2016.

765 Reddington, C. L., Spracklen, D. V., Artaxo, P., Ridley, D. A., Rizzo, L. V. and Arana, A.:  
 766 Analysis of particulate emissions from tropical biomass burning using a global aerosol model  
 767 and long-term surface observations, *Atmos. Chem. Phys.*, 16(17), 11083–11106,  
 768 doi:10.5194/acp-16-11083-2016, 2016.

769 Riahi, K., Rao, S., Krey, V., Cho, C., Chirkov, V., Fischer, G., Kindermann, G., Nakicenovic, N.  
 770 and Rafaj, P.: RCP 8.5-A scenario of comparatively high greenhouse gas emissions, *Clim.*  
 771 *Change*, 109(1), 33–57, doi:10.1007/s10584-011-0149-y, 2011.

772 Schulz, M., Textor, C., Kinne, S., Balkanski, Y., Bauer, S., Bernsten, T., Berglen, T., Boucher,  
 773 O., Dentener, F., Guibert, S., Isaksen, I. S. a., Iversen, T., Koch, D., Kirkevåg, A., Liu, X.,  
 774 Montanaro, V., Myhre, G., Penner, J. E., Pitari, G., Reddy, S., Seland, Ø., Stier, P. and  
 775 Takemura, T.: Radiative forcing by aerosols as derived from the AeroCom present-day and pre-  
 776 industrial simulations, *Atmos. Chem. Phys.*, 6, 5225–5246, doi:10.5194/acpd-6-5095-2006,  
 777 2006.

778 Smith, K. R., Bruce, N., Balakrishnan, K., Adair-Rohani, H., Balmes, J., Chafe, Z., Dherani, M.,  
 779 Hosgood, H. D., Mehta, S., Pope, D. and Rehfuess, E.: Millions Dead: How Do We Know and  
 780 What Does It Mean? Methods Used in the Comparative Risk Assessment of Household Air  
 781 Pollution, *Annu. Rev. Public Health*, 35(1), 185–206, doi:10.1146/annurev-publhealth-032013-  
 782 182356, 2014.

783 Spracklen, D. V., Jimenez, J. L., Carslaw, K. S., Worsnop, D. R., Evans, M. J., Mann, G. W.,  
 784 Zhang, Q., Canagaratna, M. R., Allan, J., Coe, H., McFiggans, G., Rap, A. and Forster, P.:  
 785 Aerosol mass spectrometer constraint on the global secondary organic aerosol budget, *Atmos.*  
 786 *Chem. Phys.*, 11(23), 12109–12136, doi:10.5194/acp-11-12109-2011, 2011a.

787 Spracklen, D. V., Carslaw, K. S., Pöschl, U., Rap, A. and Forster, P. M.: Global cloud  
 788 condensation nuclei influenced by carbonaceous combustion aerosol, *Atmos. Chem. Phys.*,  
 789 11(17), 9067–9087, doi:10.5194/acp-11-9067-2011, 2011b.

790 Stohl, A., Aamaas, B., Amann, M., Baker, L. H., Bellouin, N., Bernsten, T. K., Boucher, O.,  
 791 Cherian, R., Collins, W., Daskalakis, N., Dusinska, M., Eckhardt, S., Fuglestad, J. S., Harju,  
 792 M., Heyes, C., Hodnebrog, Hao, J., Im, U., Kanakidou, M., Klimont, Z., Kupiainen, K., Law, K.

793 S., Lund, M. T., Maas, R., MacIntosh, C. R., Myhre, G., Myriokefalitakis, S., Oliv  , D., Quaas,  
 794 J., Quennehen, B., Raut, J. C., Rumbold, S. T., Samset, B. H., Schulz, M., Seland, Shine, K. P.,  
 795 Skeie, R. B., Wang, S., Yttri, K. E. and Zhu, T.: Evaluating the climate and air quality impacts of  
 796 short-lived pollutants, *Atmos. Chem. Phys.*, 15(18), 10529–10566, doi:10.5194/acp-15-10529-  
 797 2015, 2015.

798 Streets, D. G., Yan, F., Chin, M., Diehl, T., Mahowald, N., Schultz, M., Wild, M., Wu, Y. and  
 799 Yu, C.: Anthropogenic and natural contributions to regional trends in aerosol optical depth,  
 800 1980-2006, *J. Geophys. Res. Atmos.*, 114(14), 1–16, doi:10.1029/2008JD011624, 2009.

801 Textor, C., Schulz, M., Guibert, S., Kinne, S., Balkanski, Y., Bauer, S., Bernsten, T., Berglen, T.,  
 802 Boucher, O., Chin, M., Dentener, F., Diehl, T., Easter, R., Feichter, H., Fillmore, D., Ghan, S.,  
 803 Ginoux, P., Gong, S., Grini, A., Hendricks, J., Horowitz, L., Huang, P., Isaksen, I., Iversen, I.,  
 804 Kloster, S., Koch, D., Kirkev  g, A., Kristjansson, J. E., Krol, M., Lauer, A., Lamarque, J. F., Liu,  
 805 X., Montanaro, V., Myhre, G., Penner, J., Pitari, G., Reddy, S., Seland,   , Stier, P., Takemura,  
 806 T. and Tie, X.: Analysis and quantification of the diversities of aerosol life cycles within  
 807 AeroCom, *Atmos. Chem. Phys.*, 6(7), 1777–1813, doi:10.5194/acp-6-1777-2006, 2006.

808 Tilmes, S., Lamarque, J. F., Emmons, L. K., Kinnison, D. E., Ma, P. L., Liu, X., Ghan, S.,  
 809 Bardeen, C., Arnold, S., Deeter, M., Vitt, F., Ryerson, T., Elkins, J. W., Moore, F., Spackman, J.  
 810 R. and Val Martin, M.: Description and evaluation of tropospheric chemistry and aerosols in the  
 811 Community Earth System Model (CESM1.2), *Geosci. Model Dev.*, 8(5), 1395–1426,  
 812 doi:10.5194/gmd-8-1395-2015, 2015.

813 Venkataraman, C., Habib, G., Eiguren-Fernandez, A., Miguel, A. H. and Friendlander, S. K.:  
 814 Residential Biofuels in South Asia: Carbonaceous Aerosol Emissions and Climate Impacts,  
 815 *Science*, 307(5714), 1454–1456, doi:10.1126/science.1104359, 2005.

816 Venkataraman, C., Sagar, A. D., Habib, G., Lam, N. and Smith, K. R.: The Indian National  
 817 Initiative for Advanced Biomass Cookstoves: The benefits of clean combustion, *Energy Sustain.*  
 818 *Dev.*, 14(2), 63–72, doi:10.1016/j.esd.2010.04.005, 2010.

819 Wang, Q., Jacob, D. J., Fisher, J. A., Mao, J., Leibensperger, E. M., Carouge, C. C., Le Sager, P.,  
 820 Kondo, Y., Jimenez, J. L., Cubison, M. J. and Doherty, S. J.: Sources of carbonaceous aerosols

821 and deposited black carbon in the Arctic in winter-spring: Implications for radiative forcing,  
822 *Atmos. Chem. Phys.*, 11(23), 12453–12473, doi:10.5194/acp-11-12453-2011, 2011.

823 Wang, Q., Jacob, D. J., Spackman, J. R., Perring, A. E., Schwarz, J. P., Moteki, N., Marais, E.  
824 A., Ge, C., Wang, J. and Barrett, S. R. H.: Global budget and radiative forcing of black carbon  
825 aerosol: Constraints from pole-to-pole (HIPPO) observations across the Pacific, *J. Geophys.*  
826 *Res.*, 119(1), 195–206, doi:10.1002/2013JD020824, 2014a.

827 Wang, X., Heald, C. L., Ridley, D. A., Schwarz, J. P., Spackman, J. R., Perring, A. E., Coe, H.,  
828 Liu, D. and Clarke, A. D.: Exploiting simultaneous observational constraints on mass and  
829 absorption to estimate the global direct radiative forcing of black carbon and brown carbon,  
830 *Atmos. Chem. Phys.*, 14(20), 10989–11010, doi:10.5194/acp-14-10989-2014, 2014b.

831 Ward, D. S., Kloster, S., Mahowald, N. M., Rogers, B. M., Randerson, J. T. and Hess, P. G.: The  
832 changing radiative forcing of fires: global model estimates for past, present and future, *Atmos.*  
833 *Chem. Phys.*, 12, 10857–10886, doi:10.5194/acp-12-10857-2012, 2012.

834 Zhang, L., Henze, D. K., Grell, G. A., Carmichael, G. R., Bousserez, N., Zhang, Q., Torres, O.,  
835 Ahn, C., Lu, Z., Cao, J. and Mao, Y.: Constraining black carbon aerosol over Asia using OMI  
836 aerosol absorption optical depth and the adjoint of GEOS-Chem, *Atmos. Chem. Phys.*, 15(18),  
837 10281–10308, doi:10.5194/acp-15-10281-2015, 2015.

838 Zhang, Q., Jimenez, J. L., Canagaratna, M. R., Allan, J. D., Coe, H., Ulbrich, I., Alfarra, M. R.,  
839 Takami, A., Middlebrook, A. M., Sun, Y. L., Dzepina, K., Dunlea, E., Docherty, K., DeCarlo, P.  
840 F., Salcedo, D., Onasch, T., Jayne, J. T., Miyoshi, T., Shimojo, A., Hatakeyama, S., Takegawa,  
841 N., Kondo, Y., Schneider, J., Drewnick, F., Borrmann, S., Weimer, S., Demerjian, K., Williams,  
842 P., Bower, K., Bahreini, R., Cottrell, L., Griffin, R. J., Rautiainen, J., Sun, J. Y., Zhang, Y. M.  
843 and Worsnop, D. R.: Ubiquity and dominance of oxygenated species in organic aerosols in  
844 anthropogenically-influenced Northern Hemisphere midlatitudes, *Geophys. Res. Lett.*, 34(13), 1–  
845 6, doi:10.1029/2007GL029979, 2007.

846 Zheng, Y., Unger, N., Hodzic, A., Emmons, L., Knote, C., Tilmes, S., Lamarque, J. F. and Yu,  
847 P.: Limited effect of anthropogenic nitrogen oxides on Secondary Organic Aerosol formation,  
848 *Atmos. Chem. Phys.*, 15(23), 23231–23277, doi:10.5194/acpd-15-23231-2015, 2015.

849

850 **Table 1. Annual budget for various species for the BASE, GBLSF\_OFF and INDSF\_OFF**  
 851 **simulations for the year 2010.**

Specie	ECLIPSE V5a (BASE) <sup>a</sup>	GBLSF_OFF <sup>a</sup>	INDSF_OFF <sup>a</sup>
BC	7.23	4.92	6.87
POM	18.9	8.53	17.2
SO <sub>2</sub>	98.5	97.1	98.37
NO <sub>x</sub>	120.5	118	119.8
VOC	81.1	52.4	76.6
CO	548	358	516
NH <sub>3</sub>	54.9	54.6	54.87

852 <sup>a</sup>Units are Tg specie/yr.

853

854

855

856

857

858

859

860

861



862

863 **Table 2. Model experiments setup.**

Experiments	Anthropogenic emission scenario
BASE	ECLIPSE V5a
GBLSF_OFF	ECLIPSE V5a excluding global solid fuel cookstove emissions
INDSF_OFF	ECLIPSE V5a excluding Indian solid fuel cookstove emissions

864

865

866

867

868

869

870

871

872

873

874

875

876

877

878 **Table 3. Global budgets, burden and lifetime of BC and POM from model control**  
 879 **simulations.**

Specie	BC	POM
Sources (Tg specie/yr)	9.73	49.9
fossil fuel and biofuel	7.23	18.9
biomass burning emissions	2.5	31
Sinks (Tg specie/yr)	9.72	49.8
Dry Deposition	1.8	8.14
Wet Deposition	7.92	41.7
Burden (Tg) <sup>a</sup>	0.12 $\pm$ 0.001	0.66 $\pm$ 0.006
Lifetime (days) <sup>a</sup>	4.5 $\pm$ 0.04	4.8 $\pm$ 0.04

880 <sup>a</sup>standard deviation represents the uncertainty error owing to temporal variability in the  
 881 model.

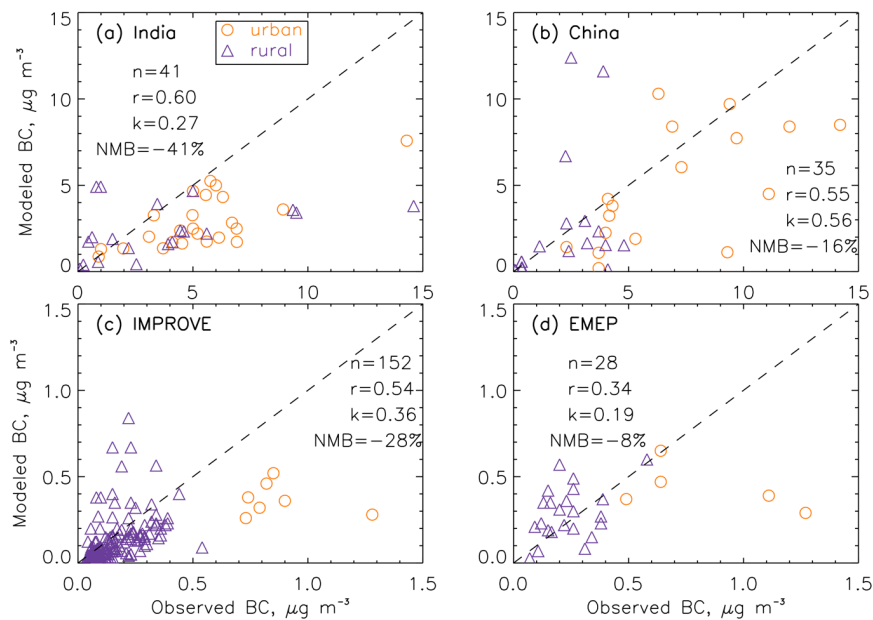
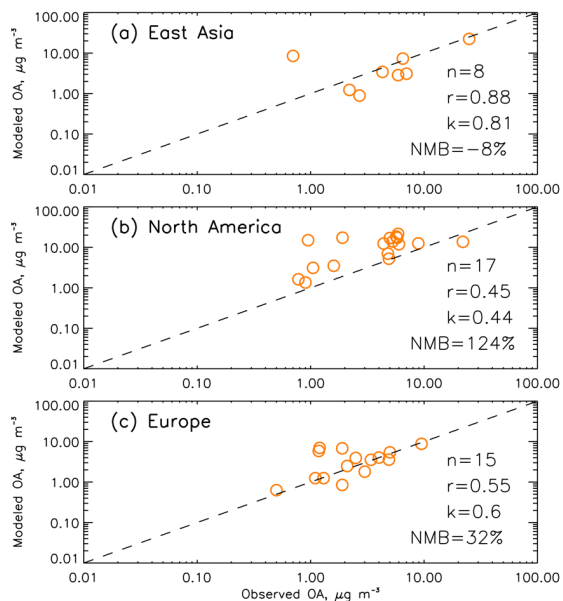


**Figure 1.** Comparisons of observational and model simulated annual mean surface BC concentrations from (a) India, (b) China, (3) IMPROVE, and (d) EMEP. Urban and rural sites are shown in orange circles and blue triangles for each region. For each panel, the total number of observational sites (n), model-to-observation regression slopes (k), correlation coefficient (r) and NMB values are included. The dashed line in each panel represents the 1:1 ratio.

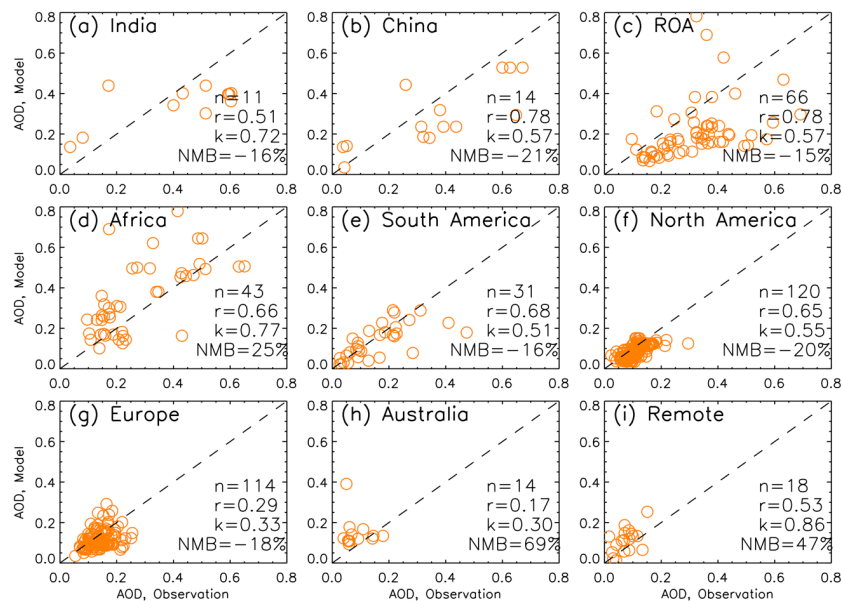


900

901 **Figure 2.** Comparisons of observational and model simulated surface OA concentrations from (a)  
 902 East Asia, (b) North America, and (3) Europe. For each panel, the total number of observational  
 903 sites ( $n$ ), model-to-observation regression slopes ( $k$ ), correlation coefficient ( $r$ ) and NMB values  
 904 are included. The dashed line in each panel represents the 1:1 ratio.

905

906



907

908 **Figure 3.** Scatter plots of AOD between model simulation and observations over (a) India, (b)  
 909 China, (c) Rest of Asia (ROA), excluding China and India, (d) Africa, (e) South America, (f) North  
 910 America, (g) Europe, (h) Australia and (i) Remote. For each panel, the total number of  
 911 observational sites ( $n$ ), model-to-observation regression slopes ( $k$ ), correlation coefficient ( $r$ ) and  
 912 NMB are included.

913

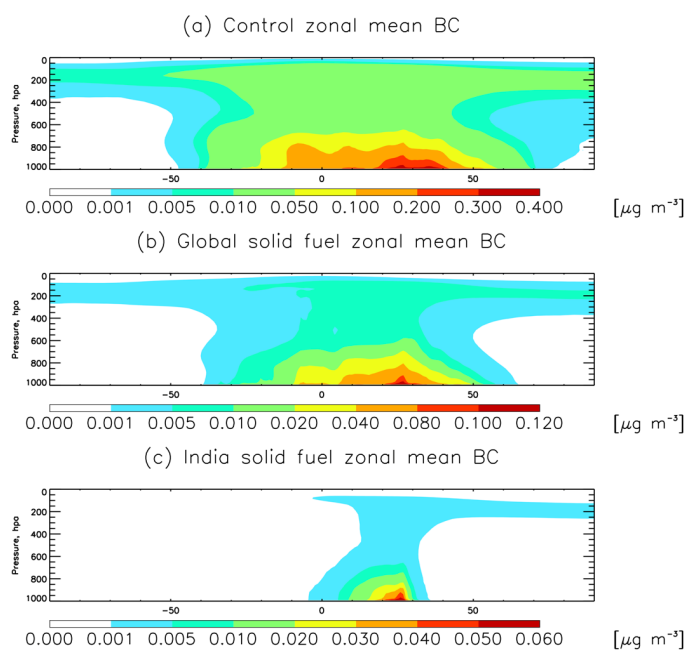


**Figure 4.** Annual zonal mean BC concentrations from (a) the BASE simulation, (b) the global and (c) India solid fuel cookstove emissions. BC concentrations are calculated under standard temperature and pressure conditions (273 K, 1 atm).

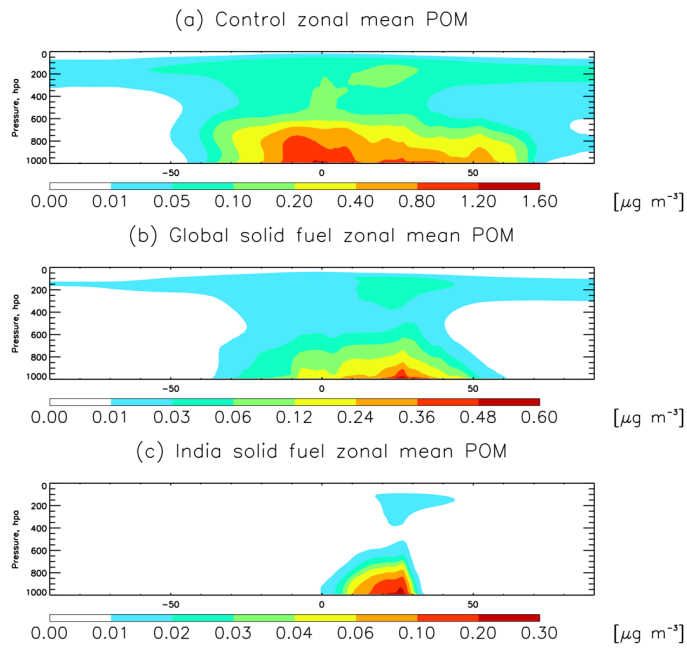


**Figure 5.** Same as Fig. 4 but for POM.

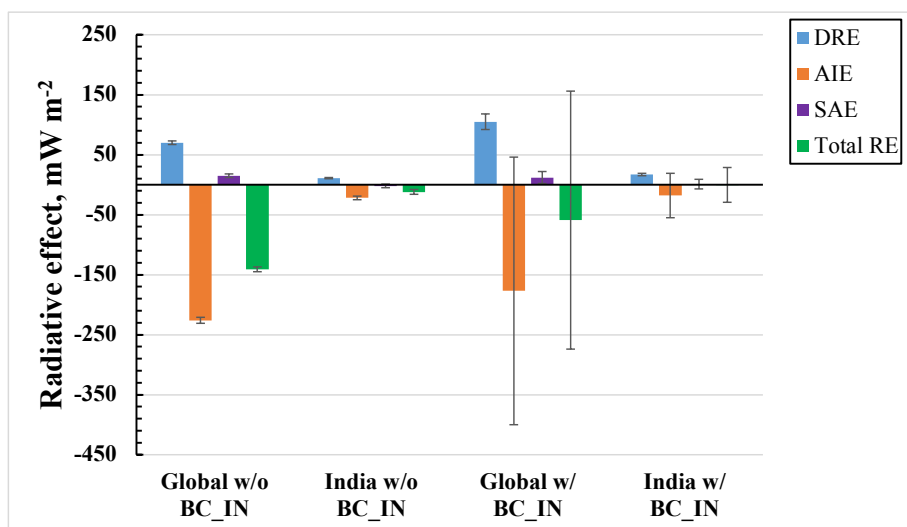


**Figure 6.** Radiative effect (RE) for global and Indian solid fuel cookstove aerosol emissions with BC not serving as IN (w/o BC\_IN) and BC as IN (BC\_IN), with DRE (blue), AIE (orange), SAE (purple) and total RE (green). Error bars represent one standard deviation for each RE. For BC as IN, standard deviations of RE are solely based on the choices of maximum freezing efficiency of BC as 0.01, 0.05 and 0.1 respectively.



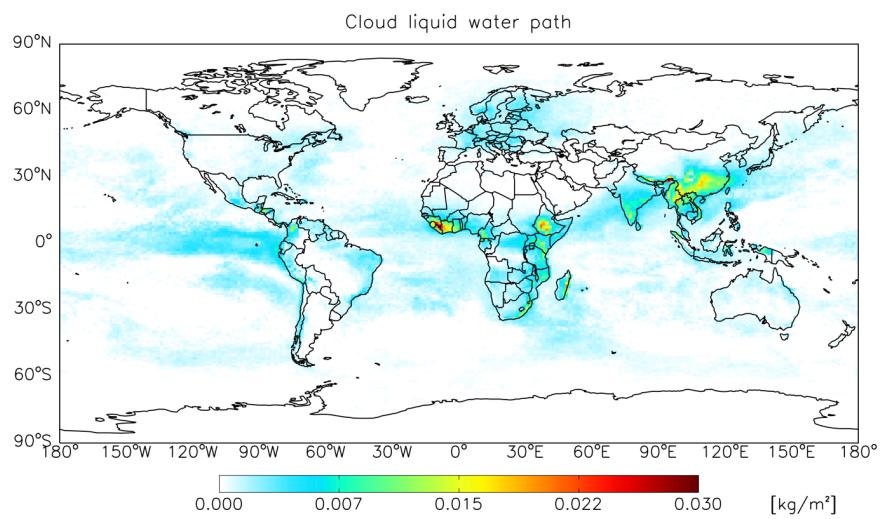


**Figure 7.** Global vertically-integrated cloud liquid water path from the global solid fuel cookstove emissions.

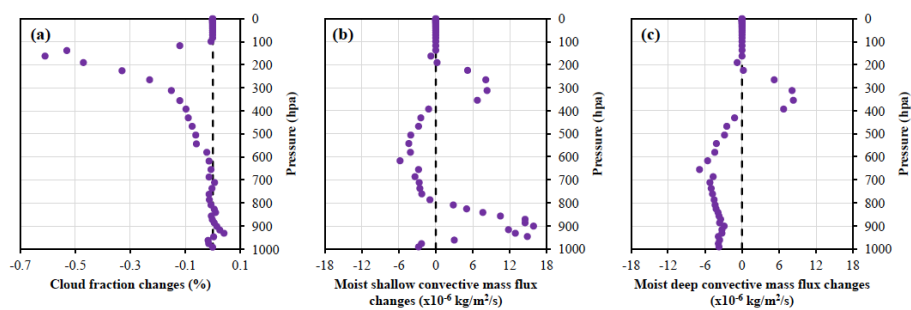


**Figure 8.** Changes in vertical cloud fractions (a), shallow (b) and deep (c) convective mass flux within the India and Indian Ocean domain from global solid fuel cookstove emissions.

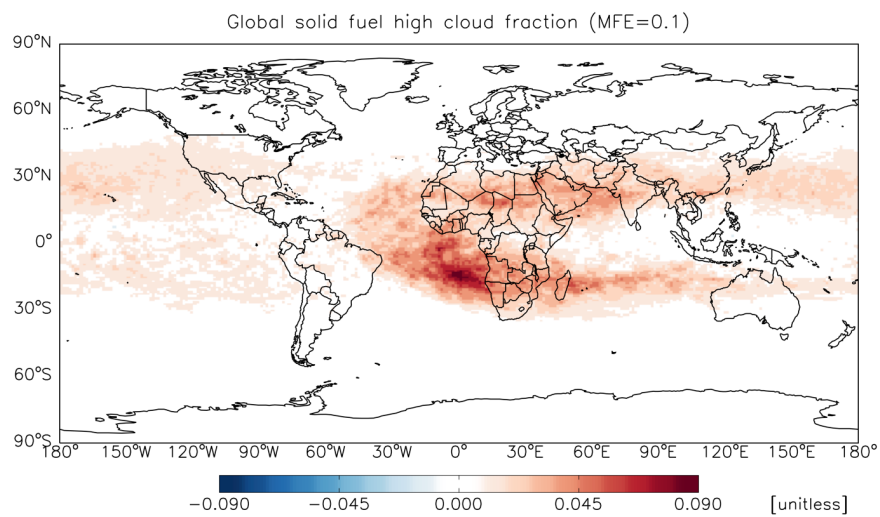


**Figure 9.** Global distribution of high cloud fraction due to solid fuel cookstove aerosol emissions with BC as IN and MFE=0.1.

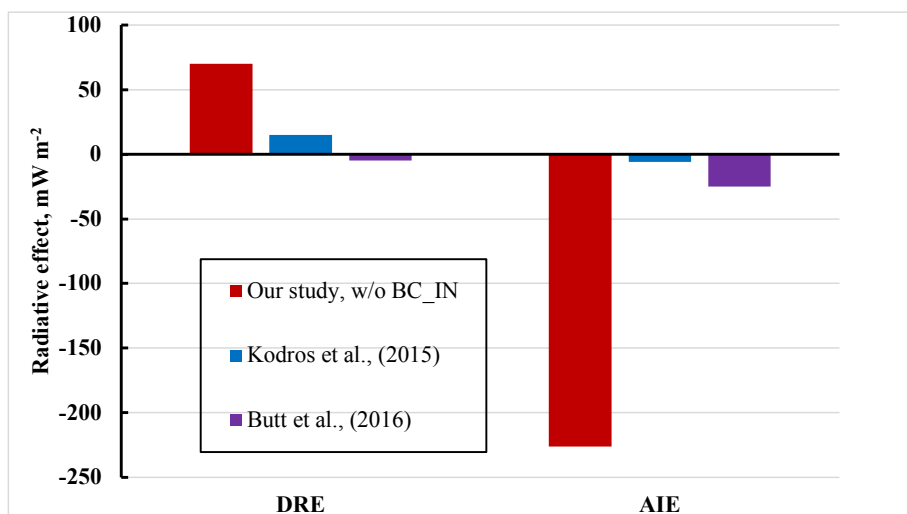


**Figure 10.** Comparisons of DRE (left) and AIE (right) radiative effects from global solid fuel cookstove emissions in our control simulation with Kodros et al. (2015) and Butt et al. (2016).